



ELSEVIER

Tectonophysics 313 (1999) 187–218

TECTONOPHYSICS

www.elsevier.com/locate/tecto

Mechanical significance of structural patterns identified by remote sensing studies: a multiscale analysis of tectonic structures in Crimea

Aline Saintot*, Jacques Angelier, Jean Chorowicz

Département de Géotectonique, U.P.R.E.S.A. 7072, Université Pierre et Marie Curie, case 129, T.25–26 E1, 4 Place Jussieu, 75252 Paris cedex 05, France

Received 12 November 1997; accepted 16 April 1998

Abstract

Based on remote sensing analyses of two panchromatic Spot scenes that cover the western and eastern parts of Crimea, completed with the study of Landsat Thematic Mapper scenes and local aerial photographs, we determined the geometry of major structures (folds and fractures). The strikes of large fractures are quite homogeneous in the studied area: three important sets are common, N10, NE–SW and NW–SE. Two strikes are particularly developed in the western part of Crimea: N25 and N105. Along important faults, we recognised the sense of motion, which often corresponds to the latest or to the major stages of movement. We also determined stress tensors by inversion of microtectonic data sets collected in the field. Combining remote sensing analysis with mechanical studies provides new views on the structural evolution of Crimea. We thus characterised major tectonic events responsible for most of the deformation. In eastern Crimea, the structural patterns fit well with two major tectonic events. (1) The latest one is a Plio–Quaternary faulting event (normal slip along N10 faults and strike-slip motion along N10 and NW–SE faults) corresponding to a transtensional regime, with σ_3 trending E–W. (2) Large fractures (NW–SE and NE–SW sets) and fold-and-thrust development reveal a transpressional regime, with σ_1 trending NNE–SSW during the Berriasian. In western Crimea, we characterised a more complex pattern of four major tectonic events. (1) The Plio–Quaternary tectonic phase induced left-lateral displacement along NW–SE faults and normal slip along WSW–ENE faults and this deformation is in agreement with the strike-slip regime that we reconstructed with σ_3 trending NNE–SSW. (2) As for eastern Crimea, the Berriasian phase was well expressed, with folds, thrusts and strike-slip faults, under a transpressional regime with σ_1 trending N–S to NNW–SSE. The two other events well identified in western Crimea are: (3) a N–S-directed extension that developed large N105 faults, and (4) a NW–SE-directed extension (involving NE–SW normal faults) that we relate to the development of peripheral troughs in the Oligocene. Western Crimea suffered a more complicated structural evolution than eastern Crimea. From eastern to western Crimea, we also noticed the systematic deviation in the trends of the principal stress axes of the recent stress field and in the Berriasian stress field as well. These differences may be related to the presence of a major crustal discontinuity: the transverse Alushta–Simferopol fault. © 1999 Elsevier Science B.V. All rights reserved.

Keywords: brittle tectonics; structures; mountain belt; remote sensing; Crimea

*Corresponding author. Present address: Vrije Universiteit, Fac. Aardwetenschappen, De Boelelaan 1085, 1081 HV Amsterdam, Netherlands. Tel.: +31-20-4447410; Fax: +31-20-6462457; E-mail: saia@geo.vu.nl

1. Introduction

As an additional tool in geological mapping, remote sensing techniques proved useful for a better description and interpretation of the geometry of major structures in mountain belts. On the other hand, palaeostress analysis based on mechanical analysis of brittle features allows accurate reconstruction of tectonic regimes in terms of nature (strike-slip, normal and reverse regimes) and orientations of stress axes. Combining these different approaches has the potential to yield better characterisation of major tectonic events, for both the structural expression and the overall mechanism.

However, it is not obvious to correlate palaeostress reconstructions and development of large-scale structures. More explicitly, because the palaeostress evolution is mainly reconstructed from minor structures and commonly polyphase, it is often difficult to determine whether a given reconstructed palaeostress regime corresponds to a minor or major tectonic episode. In terms of geodynamic evolution, the major tectonic events deserve more consideration than the minor ones. As a consequence, specific approaches are needed to determine the regimes responsible for the development and deformation of large units in a mountain belt, among the numerous tectonic regimes identified at various sites. We thus claim that remote sensing studies and palaeostress analyses should not be carried out independently, but need to be combined in order to reliably determine which mechanisms are related to the major structures.

In this paper, we consider regional aspects of the structural geology in Crimea (Ukraine). We aim at demonstrating that the reconstructed palaeostress regimes and some large structures do not solely reflect the late Cenozoic tectonic evolution. Instead, in many cases, they reveal earlier tectonics — Mesozoic or early Cenozoic. This confirms that despite the importance of the neotectonic evolution, the palaeostress analysis, combined with remote sensing mapping, also has a strong potential to allow reconstruction of the tectonic history for long geological periods in a mountain belt.

2. Geological framework: Crimea

Crimea belongs to the southern deformed boundary of the East European platform (Fig. 1a), located between the Scythian Plate (which belongs to the Eurasian continent) and the Black Sea area (Fig. 1a). The Crimean belt is 50 km wide and 150 km long. It is arch-shaped, with E–W structural trends in the east and NE–SW ones in the west. The southern zones of the belt lie offshore, within the margin of the Eastern Black Sea system (the Eastern Black Sea Basin s.str. and the Andrusov or Mid Black Sea Ridge, Fig. 1a). Major deformation within the belt occurred during the ‘Cimmerian’ phases (from the Triassic–Jurassic boundary to Berriasian times), in close relation with the closure of the Palaeo-Tethys Ocean (Kazmin et al., 1986a,b). However, consequent deformation was also Alpine (during the Tertiary), related to Arabia–Eurasia convergence and to the evolution of the Neo-Tethys (Boccaletti et al., 1974; Adamia et al., 1977; Letouzey, 1977; Zonenshain and Le Pichon, 1986).

Three structural complexes have been defined in Crimea by Milejev et al. (1996, Fig. 1b). They correspond to different steps in the sedimentary and structural development (Muratov, 1960, 1969; Koronovsky and Milejev, 1974; Byzova, 1980, 1981; Khain, 1984; Milejev et al., 1992, 1996), as follows.

The Lower Complex consists of Triassic–Bathonian folded flysch series, olistostromes, calc-alkaline volcanites and molasses. It was highly deformed during the Cimmerian phases, with south-vergent folding and thrusting processes (Koronovsky and Milejev, 1974; Khain, 1984).

The Middle Complex of Crimea is composed of terranes ranging from Late Jurassic to Berriasian in age (allochthonous terranes according to Milejev et al., 1996). Major episodes of folding and thrusting occurred during Berriasian times, with south vergence and southeast vergence (Milejev et al., 1996, 1997).

The Upper Complex includes platform cover formations which range in age from late Berriasian to Eocene. Rifting occurred throughout the area in Cretaceous times and is interpreted as a back-arc process related to a major northward subduction of the northern branch of the Neo-Tethys, prevailing to the south at that time (Boccaletti et al., 1974; Adamia et al., 1977; Letouzey, 1977; Zonenshain and Le Pi-

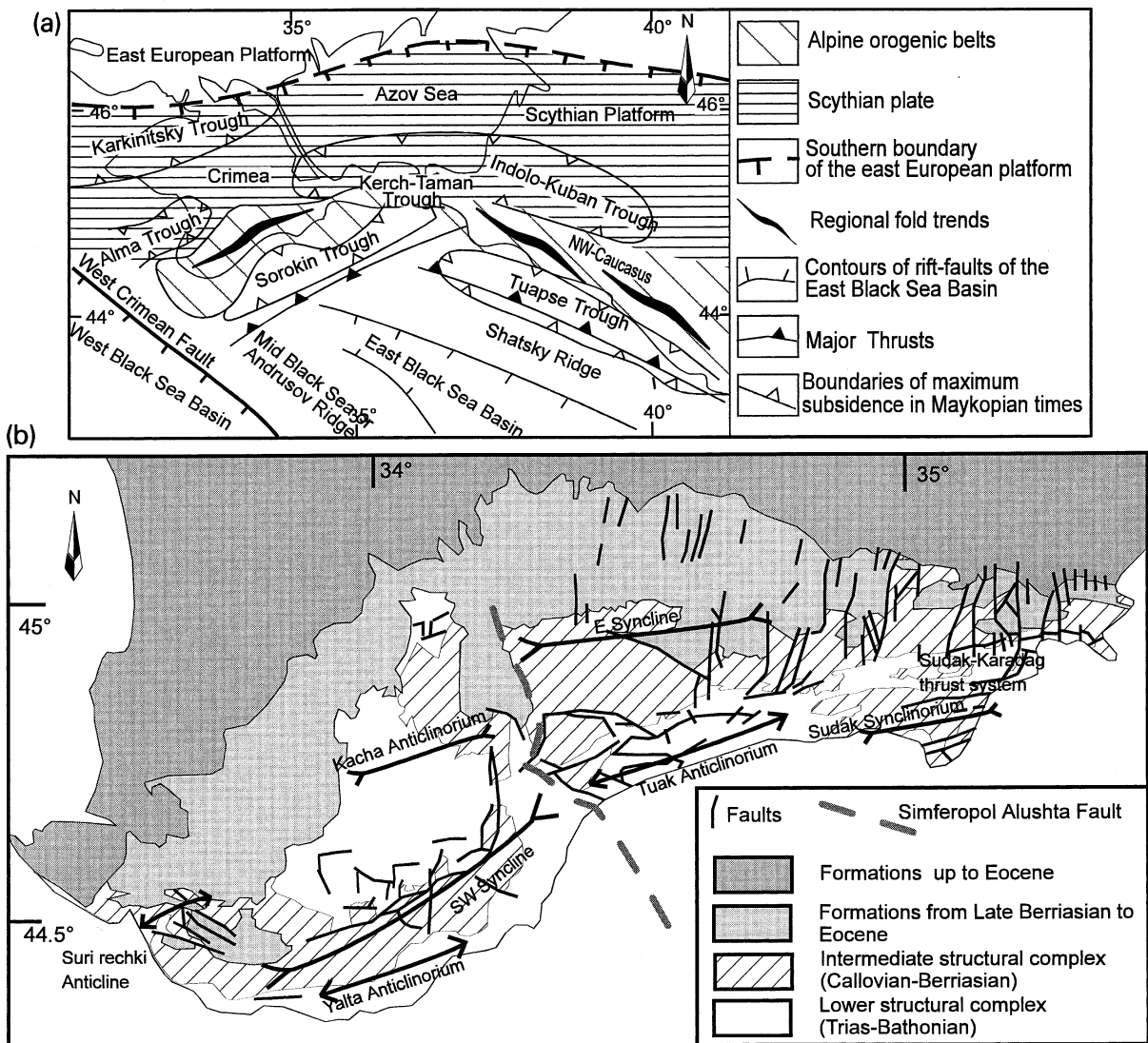


Fig. 1. (a) Structural scheme of the studied deformed belt and surrounding areas, modified from Tugolev et al. (1985), Finetti et al. (1988) and Shreider et al. (1997). (b) Structural map of Crimea compiled from Muratov (1960) and Arkhipov and Uspenskaya (1967), modified.

chon, 1986). The middle Late Cretaceous period corresponds to the development of the Western and Eastern Black Sea Basins and to rifting in the north Crimea region (Nikishin et al., 1998). According to Robinson et al. (1996) and Shreider et al. (1997), the rifting of the Eastern Black Sea Basin took place during the Paleocene to early Middle Eocene.

Most of the tectonic deformation in Crimea is concentrated in the two lower complexes, which

highlights the role of the Cimmerian phases. Following the development of these three complexes, other major tectonic events took place during the Cenozoic. Their succession can be summarised as follows. First, the Eocene–Oligocene boundary was the time of an orogenic process occurring in Crimea and the northwest Great Caucasus (Nikishin et al., 1998). Second, in the Oligocene, a strong subsidence affected most areas surrounding the Crimean

chain (Fig. 1a), i.e. the Sorokin Basin, the Alma Trough, the Indol–Kuban Basin and the Kertch–Taman transverse trough (Meysner and Tugolesov, 1981; Tugolesov et al., 1985). Nikishin et al. (1998) proposed that these troughs developed as the result of a syn-compressional process involving flexural response of the lithosphere. The surrounding deep water basins apparently formed without significant influence of extensional tectonism (Tugolesov et al., 1985; Nikishin et al., 1998) and no major extensional fault was observed on seismic profiles at the bottom of the Oligocene series (Kunin et al., 1989).

As for the more recent Cenozoic evolution, we could recognise several successive unconformities in the northern part of Crimea: (1) the unconformity of the Karaganian (Middle Miocene), (2) that of the Sarmatian (end of Middle Miocene), and (3) that of Kimmerian–Kuyalnician (Early Pliocene). These unconformities could be the result of significant tectonic events. The latest Alpine deformation induced south and SSE-vergent thrusting in the offshore part of the chain (observed by Terekhov and Shimkus, 1989, on seismic profiles), as related to incipient subduction of the East Black Sea Plate beneath the Crimea and with the collision of Crimea with the Mid Black Sea Ridge (Andrusov Ridge) following a NNW or NW displacement (McKenzie, 1972; Nowroozi, 1972; Seismotectonic Map of Iran, Afghanistan and Pakistan, 1984). As observed in seismic profiles, by Tugolesov et al. (1985) and Finetti et al. (1988), all terranes up to the Quaternary formations are affected by this latest tectonism. The seismic activity reveals that this compressional deformation is continuing.

Concerning the polyphase structural evolution of Crimea, there is some controversy between authors about the major structuration of Crimea, especially concerning the vergences of thrust sheets and the ages of their development. Mileev et al. (1997) considered the thrust sheet development as Berriasian in age with a south and southeast vergence (N160–N120 in azimuth). Popadyuk and Smirnov (1991, 1996) assumed that the thrusting in Crimea was generally north-vergent and had occurred during the Austrian phase (middle Cretaceous). Galkin et al. (1994) concluded that the allochthonous Late Jurassic rocks of the Chatyr Dag Massif overthrust terranes up to the Albian. According to Scherba (1978),

the allochthonous complex (Late Jurassic terranes) was displaced to the south in Late Cretaceous–early Palaeogene times, and the detachment surface was reactivated during the Plio–Quaternary. Kazantsev (1982) and Kazantsev et al. (1989) reported that the structural complexes are involved in north-vergent thrust sheets including rocks from the Palaeozoic to Sarmatian.

In this paper, emphasis is put on the analysis of brittle tectonics, because of the possibility to accurately reconstruct successive tectonic mechanisms. Concerning the major fracture patterns of the Crimean chain, several main faults at depth were revealed by geophysical studies. Most of them separate the Crimean belt from adjacent geological regions (Morgunov et al., 1979; Byzova, 1980; Khain, 1984; Koronovsky, 1984). The NW–SE deep fault from Alushta to Simferopol (Fig. 1b) is a major structure of Crimea with an eastward dip of the fault plane. The occurrences of Middle Jurassic intrusives are closely related to the presence of this deep fault cutting across the belt (Khain, 1984). The transverse deep fault, trending N–S and passing the east of Feodosya, corresponds to the downwarping and eastern termination of the Crimean Mountains beneath the thick Maykop deposits (Oligocene–Early Miocene in age) of the Kertch transverse trough. The northern slope of the chain is bounded by a deep fault, trending NW–SE between Sebastopol and Simferopol, and E–W east of Simferopol. Note that NE–SW directions of deep faults were recognised by Boccaletti et al. (1988), based on Landsat MSS imagery observations. To the south, the offshore part of the Crimean belt is separated from the East Black Sea Basin by a deep fault trending nearly E–W. Considering the compressional or transpressional regime which prevailed in the southern margin of Crimea during belt development, this deep fault is interpreted as a major thrust across which the Eastern Black Sea Plate is beginning to subduct under the Crimean belt (i.e. the Scythian Plate, Fig. 1a).

3. The structural pattern: insights from satellite scenes and aerial photographs

We used two panchromatic scenes acquired by the Spot satellite (Fig. 2). We also used two Land-

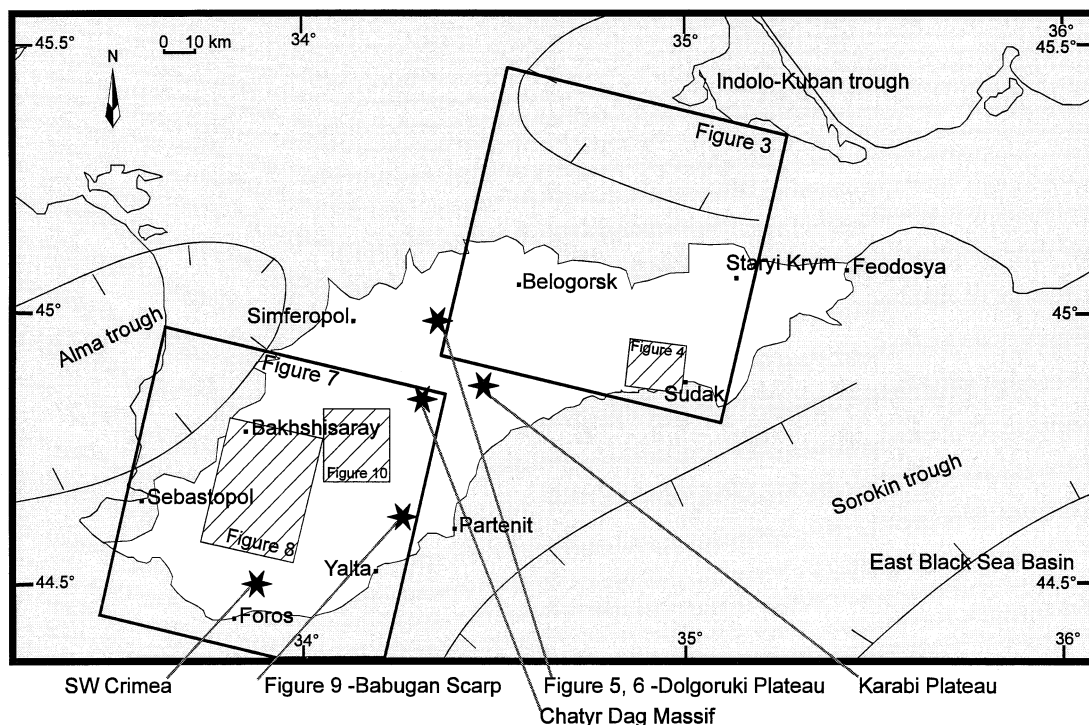


Fig. 2. Location of studied panchromatic Spot scenes (square frames) corresponding to Figs. 3 and 7, of extracted views of Spot scenes (hachured square frames) corresponding to Figs. 4, 8 and 10, and of aerial photographs (black stars) in Crimea.

sat Thematic Mapper scenes in order to cover the whole Crimean Mountains. Technical characteristics of satellite scenes are plotted in Table 1. We worked primarily with the Spot images (Fig. 2), because of their higher ground resolution (Table 1). The Landsat TM imagery was principally used as a complement

of Spot scenes in order to constitute stereoscopic couples (the difference between incidence angles of Landsat and the Spot scenes being 23° or larger). We carried out mapping analysis and fault characterisation, and systematically attempted to reconstruct the senses of displacements on faults (as in Chorowicz et

Table 1
Characteristics of used satellite scenes

	Panchromatic Spot scenes KJ: 108/260, 109/259	Landsat Thematic Mapper scene paths and rows: 177/29, 178/29
Wavebands, λ (μm)	0.51–0.73	1st band: 0.45–0.52 (visible blue) 2nd band: 0.52–0.60 (visible green) 3rd band: 0.63–0.69 (visible red) 4th band: 0.76–0.90 (near infrared) 5th band: 1.55–1.75 (mid infrared) 6th band: 10.40–12.50 (thermal infrared) 7th band: 2.08–2.35 (mid infrared)
Nominal ground resolution	10 m	30 m (bands 1 to 5 and 7) 120 m (band 6)
Coverage	60 × 60 km	185 × 170 km

al., 1994a, 1995). We recognised stratigraphic units based on the correlations with available geological maps (1/1,000,000 — Arkhipov and Uspenskaya, 1967 and 1/200,000 — Derenyuk et al., 1984) and our field work. We identified some characteristic ‘signatures’ of lithology in images. We finally paid special attention to the structural relationships between the various lithostratigraphic units of Crimea.

In some areas, aerial photographs are available at the 1/20,000 as well as 1/10,000 scales. Because of their far better resolution than for the satellite images, such aerial photographs are of extreme interest in the structural analysis. Fig. 2 presents the areas covered by aerial photographs: the Karabi, Dolgoruki and Demerdji Plateaus, the Chatyr Dag Massif, and the southwestern part of the Crimean chain (Late Jurassic terranes of the Babugan Plateau, the Yalta Plateau and Ai Petri Plateau). The analyses of these

aerial photographs allowed us to complete and better constrain the general structures that we extracted from satellite imagery.

3.1. Analysis of the satellite images of eastern Crimea (Sudak, Belogorsk, Staryi Krym)

Fig. 3 shows both the original Spot panchromatic scene (Fig. 3a) and the extracted structural interpretation (Fig. 3b).

We could observe the E–W-directed scarps of several cuestas in the northern slope of the chain. The northernmost scarp is composed of Sarmatian limestones which dip a few degrees to the north and unconformably overlie the Eocene limestones (Bakhchisaraian–Simferopolian horizons). This unconformity is clearly observable northwest of Belogorsk (Fig. 3). The Paleocene formations dip 10° to

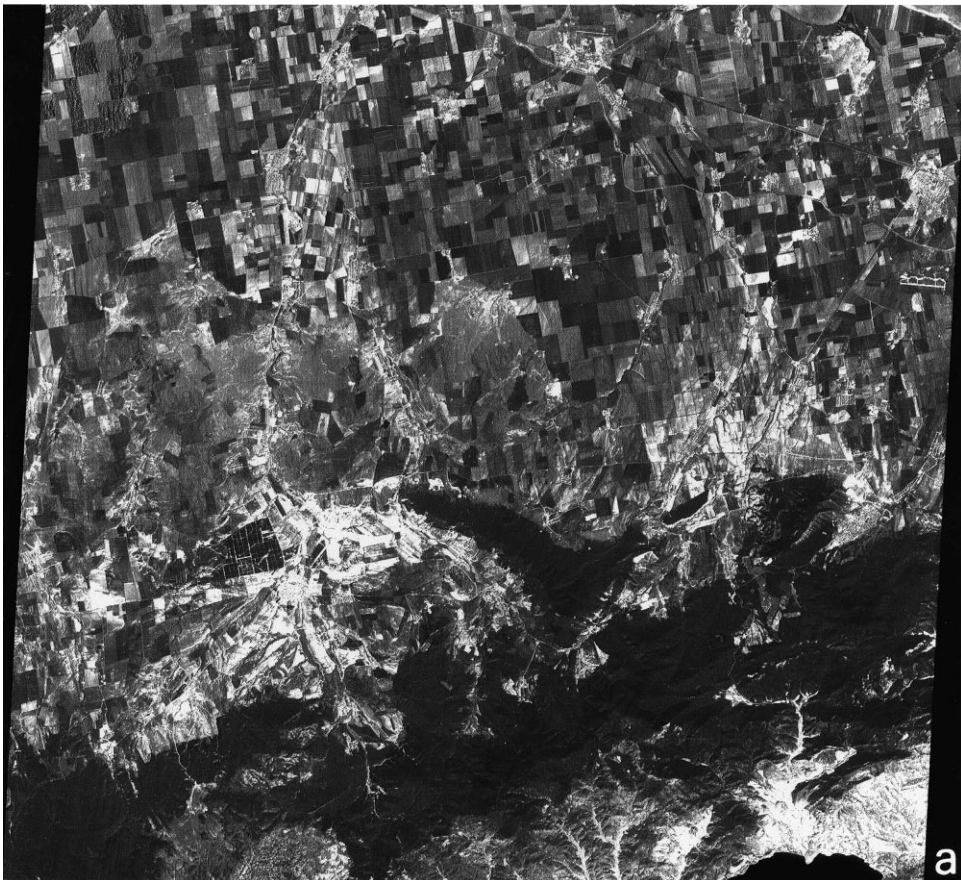


Fig. 3. Interpretation of satellite images in eastern Crimea. (a) Original Spot panchromatic scene.

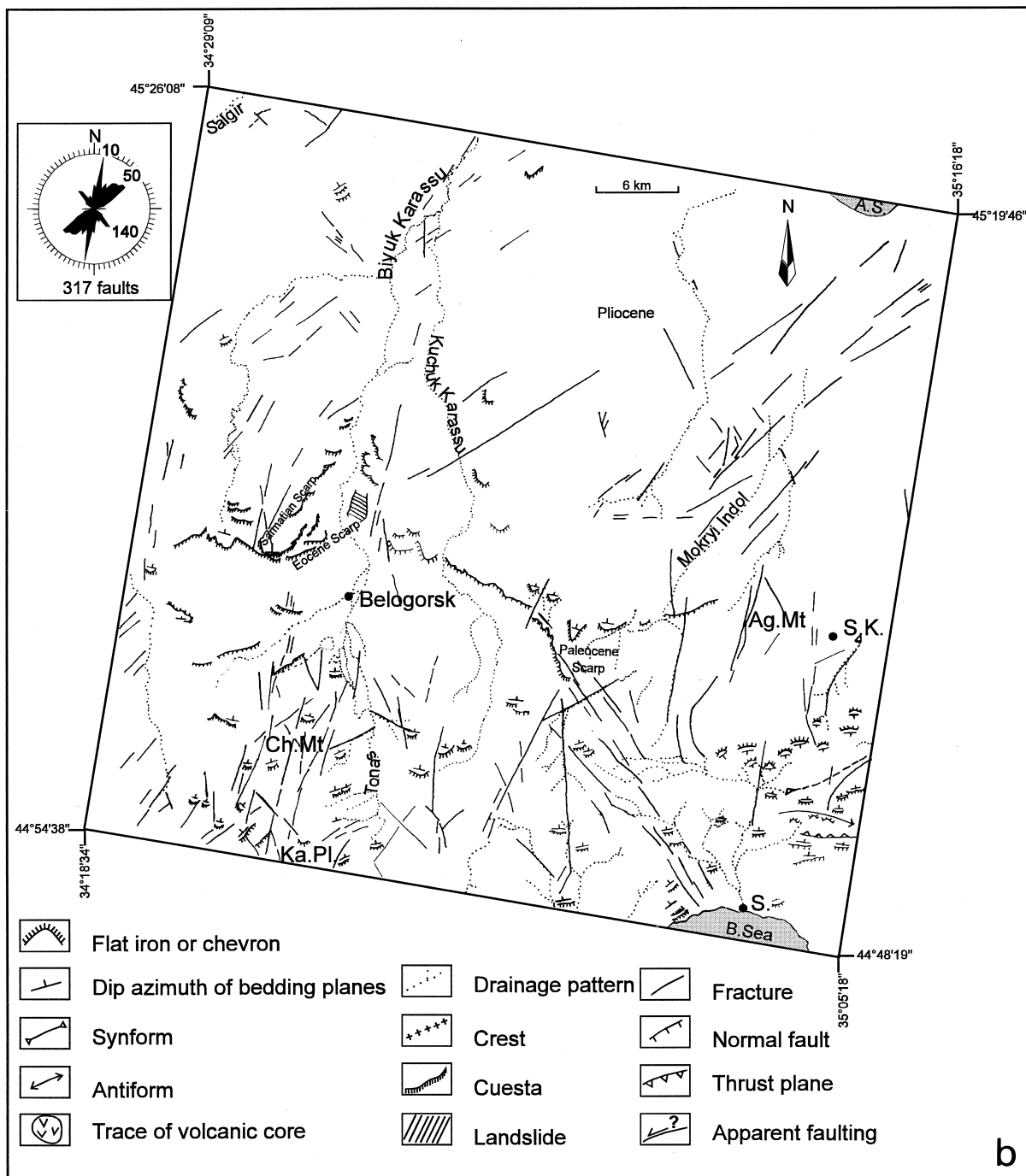


Fig. 3 (continued). (b) Corresponding structural map from analyses of Spot panchromatic–Landsat TM couples of eastern Crimea. Trend distribution of traces added in rose diagram. *S.K.* = Saryi Krym; *S.* = Sudak; *Ka. Pl.* = Karabi Plateau; *Ch. Mt.* = Chombay Mountain; *Ag. Mt.* = Agarmysh Mountain.

the north and form an important scarp well seen between Belogorsk and Staryi Krym (Fig. 3). Beneath these Cenozoic formations, the Mesozoic terranes (Fig. 3b) generally dip to the north, as indicated by the traces of bedding surfaces or by the presence of characteristic flat iron features. The accuracy of the Spot imagery is not sufficient to allow identification of unconformities in the Cretaceous terranes, because of the poorer contrasts and smoother morphologic expressions.

In the region north of Sudak, within the highly deformed Lower and Middle Complexes, we identified synform and antiform structures that we interpreted as synclines and anticlines with E–W-directed axes, suggesting a N–S direction of shortening. Furthermore, we could identify the traces of nearly E–W south-vergent thrust fronts which affect both the Lower Complex and the Middle Complex of Crimea. This area corresponds to the Sudak–Karadag thrust system (Fig. 1b). The Cretaceous terranes in the northern slope of the chain are not affected by such intense folding. This observation confirms that the major deformation with a N–S trend of shortening strictly belongs to the late Cimmerian phase (during Berriasian times).

As for the fracture patterns, we observed 317 traces of fractures in the Spot scene shown in Fig. 3, with a larger density of fracture traces in the formations belonging to the Lower and Middle Complexes of Crimea. This spatial distribution is in agreement with the tectonic evolution of Crimea mentioned before and indirectly supports the major role of Cimmerian tectonics.

The analyses of these 317 fracture lines in terms of strike (rose diagram in Fig. 3b) revealed that the predominant trend is N10. An important group also trends N50, and a minor one trends N140. We also noticed that the strikes of fractures are in agreement with the strike of deep faults bordering the belt: the N10 direction corresponds to the strike of the Feodosya fault, whereas the N140 direction fits the strike of the Alushta–Simferopol fault.

It is more difficult to characterise the offsets along faults. Because of the structural interest of such reconstruction, we addressed this problem in a systematic way. NNE–SSW- to NE–SW-striking large faults cross the belt and its foreland, affecting the Mio–Pliocene units. The drainage network

(formed by the Kuchuk Karassu, the Biyuk Karassu, the Mokryi Indol river valleys, Fig. 3b) is running along NNE–SSW and NE–SW parallel structural lines which correspond to northern prolongation of the faults that we characterised inside the mountain belt. The offsets of the Palaeogene cuestas enabled us to determine an apparent left-lateral strike slip movement along these NNE–SSW to NE–SW faults. South of Belogorsk, across the Chombay Mountain, such N–S-striking faults, steeply dipping to the east, apparently offset a crest formed by Jurassic limestones in a left-lateral sense. Vertical components were also identified, at the eastern slope of the Agarmysh Mountain, where a NNE–SSW-trending fault occurs with a downfaulted western part. Doushevsky and Lysenko (1978) determined vertical offsets of 15–35 m along these sets of faults. Inside the allochthonous Late Jurassic formations which compose the Agarmysh Mountain, such NNE–SSW fractures were identified. NW–SE faults were also identified crossing both the belt structures and the Mio–Pliocene formations of the foreland. The recent displacement along these NW–SE faults is right-lateral, as unambiguously indicated by offsets of crest line (Fig. 4). This fault pattern corresponds to the latest stage of deformation affecting the Crimean Peninsula during the Late Cenozoic.

This example illustrates both the structural interest and the limits of the remote sensing analyses. The main structural trends are identified; more accuracy is however needed in terms of structure geometry and related mechanisms.

3.2. Central Crimea: aerial coverage

Our Spot scenes (Fig. 2) do not cover the central part of the Crimean chain. However, we used aerial photographs (located in Fig. 2), which allowed us not only to obtain full coverage but also to carry out much more accurate structural analyses in the allochthonous terranes composed of Late Jurassic formations.

Part of the Dolgoruki Plateau is covered by 1/10,000 aerial photographs (Fig. 2). Analysis of the internal structure of this allochthonous complex allowed us to better observe the vergence of the thrust sheet development, as well as the later deformations. We easily characterised normal faulting, as shown by

the systematic offsets of clearly observable beds along the Tithonian scarp. NW–SE-trending normal faults thus constitute a conjugate system indicating a NE–SW extension (Fig. 5). In more detail, we observed that the joints are highlighted by strong dissolution. We also noticed the development of reverse faults, that we interpreted as compensation faults accompanying normal slip on convex faults (Fig. 5).

As for the compressional deformation revealed in these aerial photographs, and related to the thrust sheet development, accurate observations were also made. In the lower part of the Dolgoruki Plateau scarp, we recognised a level of highly deformed rocks. We observed successive asymmetrical antiforms and synforms, with E–W axes (Fig. 6). According to Milejev et al. (1996), it is a level of deformed early to middle Tithonian overthrust by undeformed formations of the same age. A criterion of relative chronology is given by the analyses of these aerial photographs. We noticed that the recumbent folds at the bottom of the scarp are strongly affected by the normal faulting that we characterised at the top of the scarp (Fig. 5).

Using a coverage of aerial photographs at a 1/10,000 scale, the internal structure of the Late Jurassic allochthonous complex was thus reconstructed. Especially, an important development of normal faults post-dated that of thrust sheets and folds.

3.3. Satellite coverage combined with local aerial coverage: structural analysis in western Crimea (Sebastopol, Bakhchisaray)

Fig. 7 shows both the Spot scene in western Crimea (Fig. 7a) and the extracted structural interpretation (Fig. 7b), with rose diagrams of observable fracture strikes. In this section, we consider together the analyses of satellite images and aerial photographs, which proved to be efficient combined tools to describe the deformation.

We noticed the spectacular NE–SW scarp of the Danian on the northwestern flank of the Crimean belt. Farther north, Sarmatian limestones compose the northernmost cuesta which unconformably overlies older terranes.

In southwestern Crimea, we recognised the well known ENE–WSW-trending syncline of southwest-

ern Crimea, composed by Jurassic formations and unconformably overlain by Early Cretaceous (Hauterivian) terranes which dip to the north and show no evidence of intense folding.

As for brittle structures, 396 fracture traces could be identified in the Spot image of west Crimea. In the rose diagrams (Fig. 7b) the azimuthal distribution reveals higher dispersion than for eastern Crimea. We identified five groups of directions: N15, N25, N45, N105 and N135. To better constrain the distribution of fracture traces, we took the length of traces into account. The groups trending N15, N25, N45 correspond to 270 fractures with lengths less than 3 km, whereas the groups striking N110, N135 include 126 fractures with lengths more than 3 km. Significantly, the strikes of these fractures are in agreement with those of deep faults bordering the belt: the N15 strike fits that of the Feodosya while the N135 fits that of the Alushta–Simferopol fault.

The drainage network in this region is consistent with the fault pattern. In the Spot scene, we noticed drainage anomalies. The Alma, Kacha and Belbek river valleys are directed SE–NW in the core of the mountains (upstream drainage), and ENE–WSW in Pliocene terranes in the northwestern back of the Sarmatian cuesta (downstream drainage). In the Pliocene formations, the ancient drainage network formed by these rivers can be identified. It followed the NW–SE (N135)-directed linear structures mentioned above. This pattern reveals a phenomenon of drainage network capture, because of northward block tilting, along ENE–WSW large faults. We confirm that vertical offsets recently occurred in Pliocene terranes along this ENE–WSW trend, as well observed in the Lower Belbek river valley by the difference in elevation between the northern and the southern blocks.

In the core of the chain, the drainage network follows NW–SE-trending faults along which there are large left-lateral displacements, as indicated by the observation of releasing bend basins in the Alma, Bodrak and Belbek valleys and as suggested by the offsets of the cuestas (Fig. 8). We observed apparent horizontal offsets of nearly 2 km affecting the Danian cuesta and the Cretaceous formations along the NW–SE fault of the Belbek river valley (Fig. 8). The ENE–WSW fault of the lower Belbek river apparently offsets a NW–SE fault in a right-lateral sense.

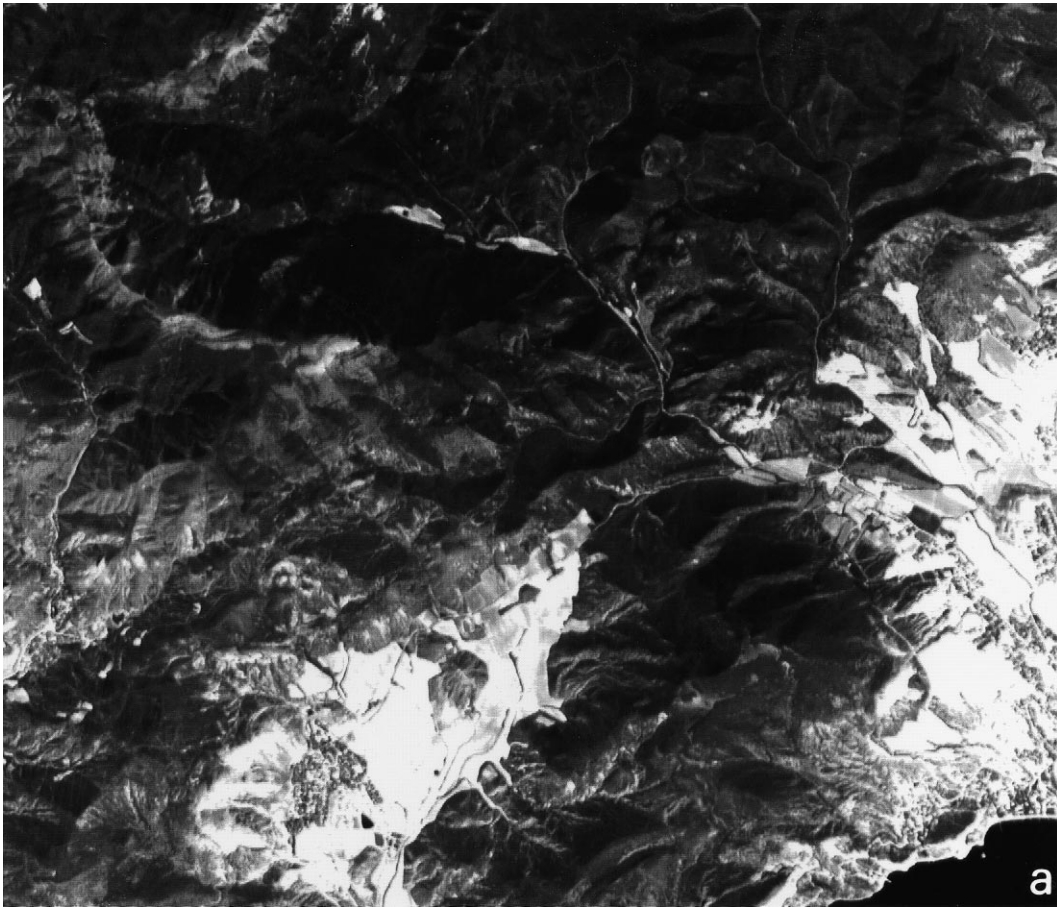


Fig. 4. Spot analysis: NW of Sudak. (a) Spot view.

This structural pattern suggests that these faults form a system of conjugate strike-slip faults, in agreement with a stress regime with E–W-trending compression and N–S-trending extension.

The high plateau of Ai Petri formed by the structural surface of Late Jurassic limestones is cut by nearly E–W plurikilometric faults (N105 set) with downthrown blocks to the south. Such normal faults are common in the whole of the southwestern Crimean chain. The available coverage of aerial photographs (1/20,000) in this area allowed us to confirm the main fault displacements recognised in satellite scenes. We especially identified a major scarp in the Ai Petri Plateau which corresponds to an E–W-striking normal fault affecting the southwestern syncline of Crimea. Along the steep southern scarp of the Babugan Plateau (aerial photograph at

1/10,000 scale, Fig. 9a), a WNW–ESE array of highly fractured Late Jurassic limestones was observed (Fig. 9b) and analyses of brittle tectonic features near this faulted zone revealed a normal faulting similar to that suspected in satellite images.

The structural pattern of the Lower Structural Complex is well observed in the Bodrak, Alma, Kossa, Kacha, Marta and Belbek river basins. The usual bedding dip direction in the terranes of the Lower Complex is north and north-northwest, as indicated by numerous flat irons but we observed numerous antiforms and synforms which complicate the structural pattern of the Lower Complex. We observed important anomalies in the shape of the drainage network of the Alma, Kossa and Bodrak upstream valleys. These anomalies are interpreted as traces of south-vergent thrusts (Fig. 7b). Both these

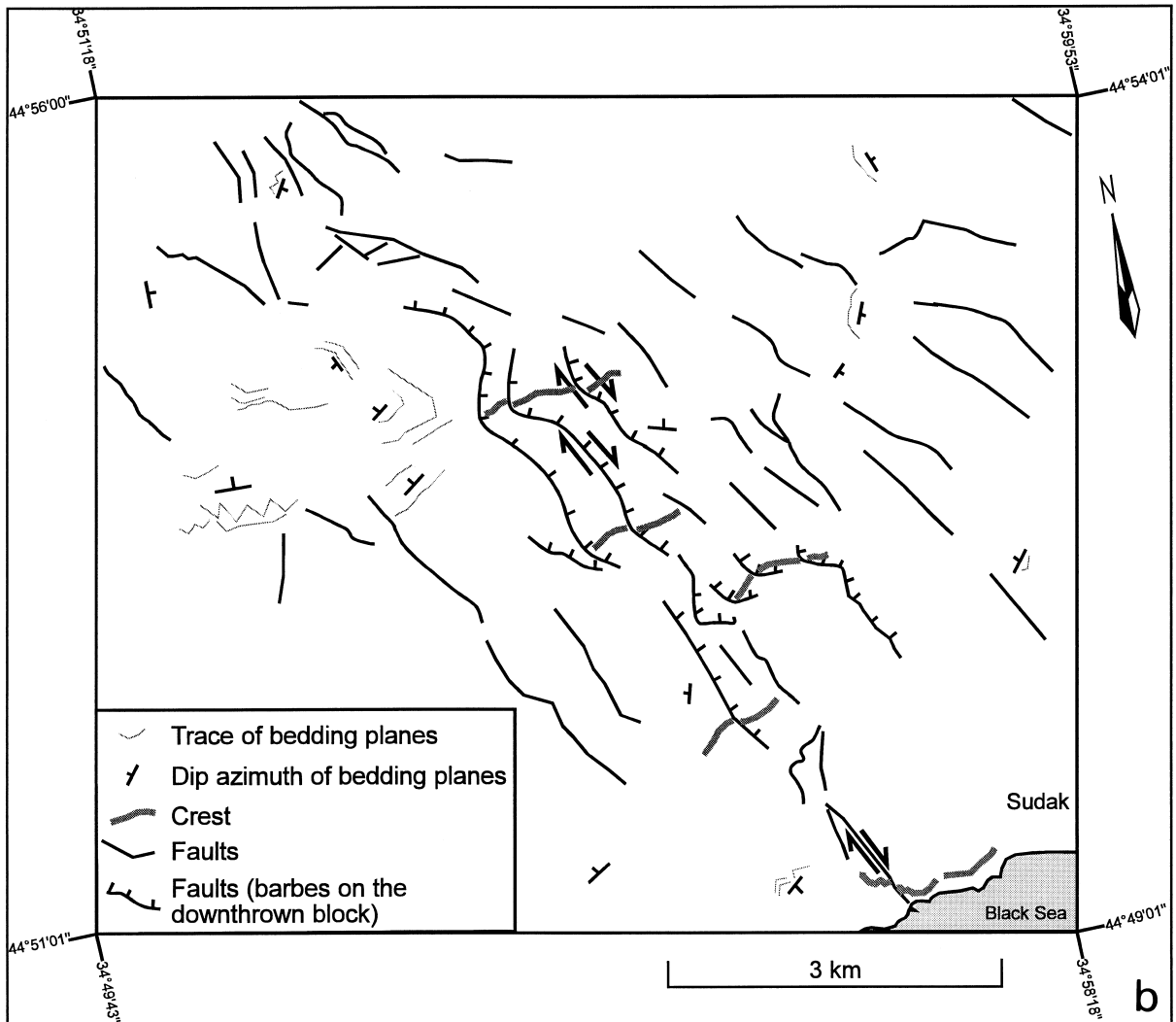


Fig. 4 (continued). (b) Local interpretation of the Spot view, NW of Sudak. Note that crest lines are offsets along NW–SE faults and that fault slips are oblique, normal and right-lateral.

observations are compatible with folding related to a N–S direction of compression. The allochthonous position of the Middle Complex, relative to the intensively deformed Lower Complex, is well identified in the vicinity of the Chatyr Dag Massif and Ai Petri Plateau (Fig. 7b). The difference of amplitude in terms of deformation between these two complexes is clearly observed and fits well the occurrence of an early phase of deformation which affected the Lower Complex, before the sheet development of the Middle Complex above the Lower Complex. This early

phase may correspond to an early Cimmerian phase during Callovian times.

We also observed anomalies in the drainage network of the upstream basin of the Alma river (Fig. 10). The pattern is clearly centrifugal and this kind of drainage anomaly is generated by circular features (Deffontaines and Chorowicz, 1991). Obert et al. (1992) observed such circular drainage anomalies in the eastern Paris Basin, which correspond to a Palaeozoic volcano buried beneath 1000 m of deposits, as indicated by a seismic cross-section.

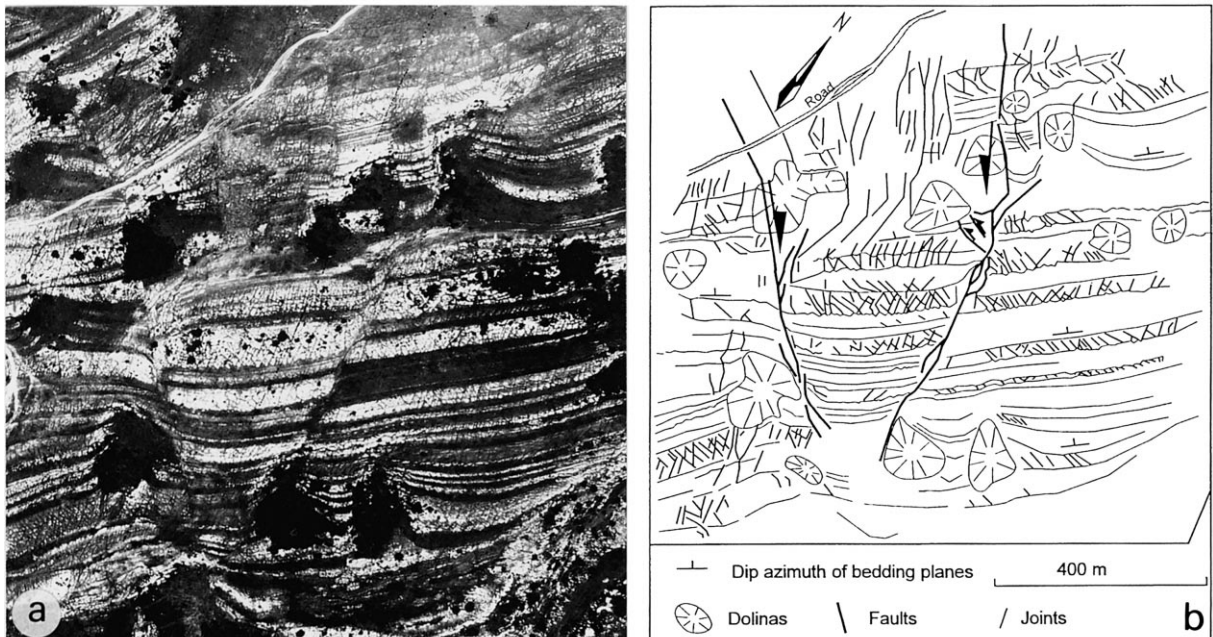


Fig. 5. Southern scarp of Dolgoruki Plateau, upper part (Tithonian deposits). (a) Aerial photograph. (b) Corresponding structural map. Note the presence of normal fault system.

We inferred that the circular anomalies in Crimea may also correspond to magmatic cores located beneath the terranes of the Lower Complex, similar to outcropping Middle Jurassic intrusives known elsewhere in Crimea.

3.4. Comparison between the structural schemes of western and eastern Crimea

Three common directions of fracturation, N10–N15, N50 and N135–N140, occurred both in eastern and western Crimea. These strikes are in agreement with the strikes of the largest deep faults revealed by geophysical data. In western Crimea, two sets of faults, N25 and N105, exist in addition.

It is important to point out that the deformation in the Lower Complex cropping out in eastern and in western Crimea is compatible with a N–S-directed compression.

Concerning the latest stage of deformation that we identified by analyses of features in Pliocene terranes of the foreland, there is an obvious counterclockwise deviation of the deformation from eastern to western Crimea. The trends of latest faulting are NNE–

SSW (N10), NE–SW (N50) and NW–SE (N140) in the eastern foreland whereas they are WNW–ESE (N105), NW–SE (N135) and ENE–WSW in the western foreland. Normal and strike-slip faulting occurred across these faults with a counterclockwise deviation of the direction of associated compression and extension.

4. Major structures in relation to palaeostress regimes

Several palaeostress regimes have been reconstructed throughout Crimea by means of brittle tectonic analysis and fault slip data inversion (Angelier et al., 1994; Saintot et al., 1995, 1996a,b). This regional analysis was based on consideration of 970 minor fault slip data and other brittle features (e.g., 290 veins, 215 stylolitic pressure-solution fractures) at 52 sites. The aim of the present paper is not to describe the regional palaeostress history (Saintot et al., 1998). We rather aim at demonstrating that the results can be correlated with the development and deformation of the large-scale structures dis-

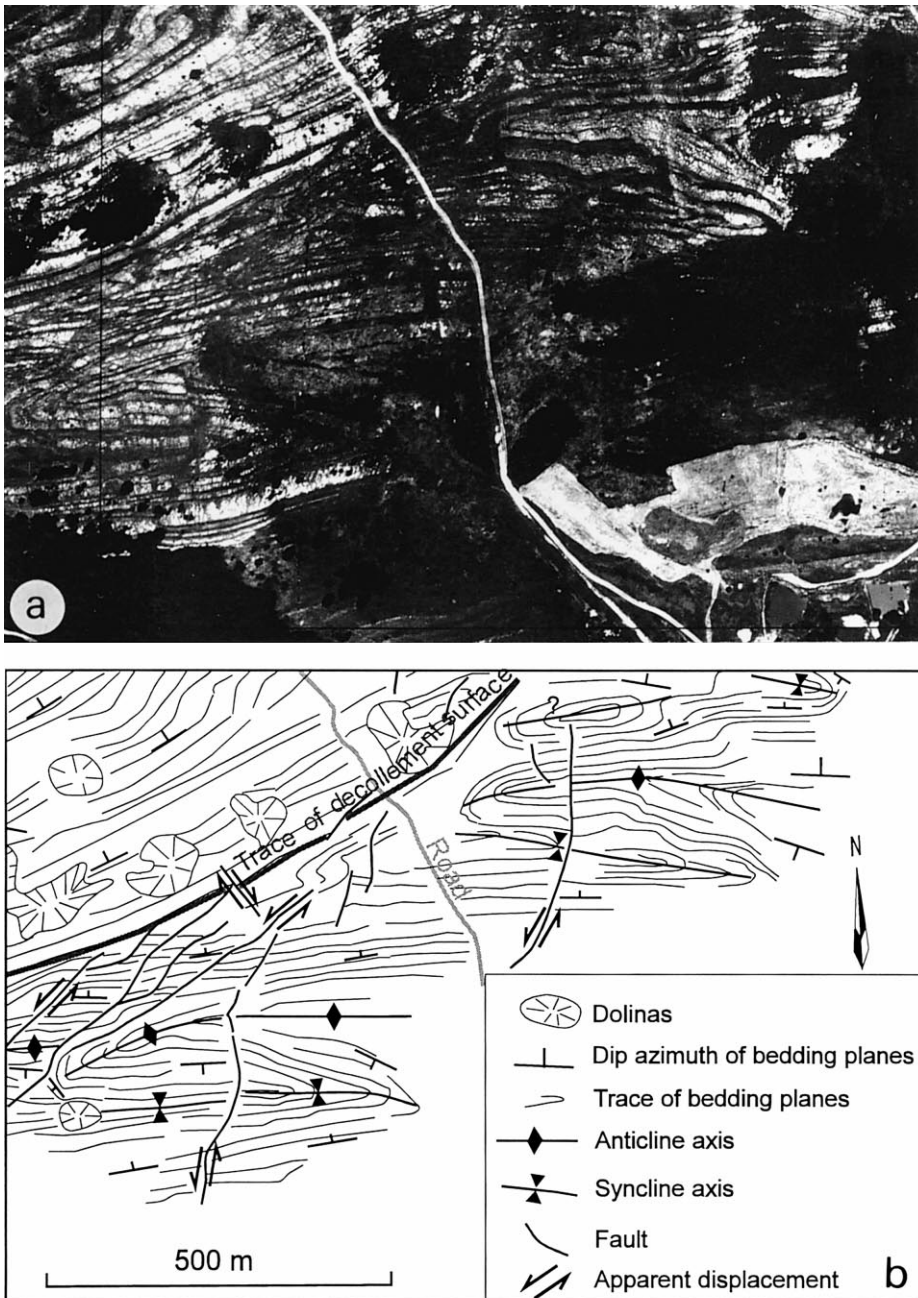


Fig. 6. Southern scarp of Dolgoruki Plateau, lower part (Tithonian deposits). (a) Aerial photograph. (b) Corresponding structural map. Note the presence of an internal thrust in the allochthonous complex and folds in the overthrust unit.

cussed above. As a consequence, we simply selected and summarised the palaeostress data and results corresponding to these major events (in detail, in

Table 2), at places where analyses of satellite images and aerial photographs yielded significant structural information.

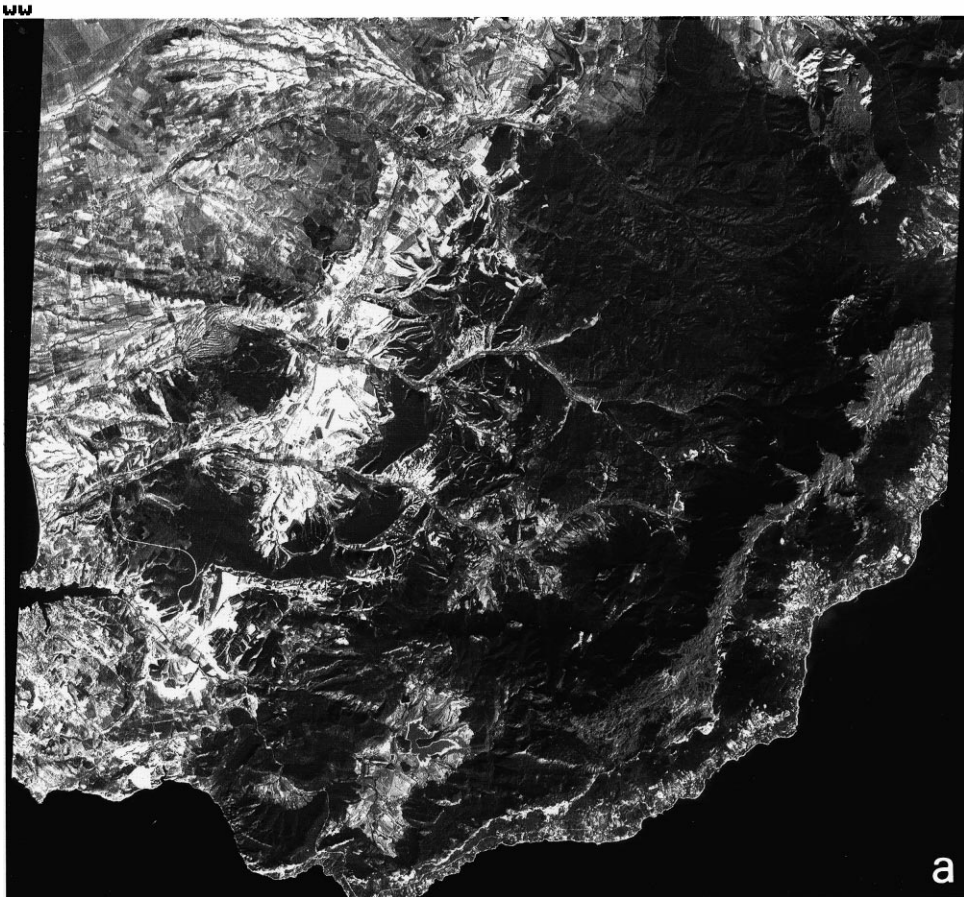


Fig. 7. Interpretation of satellite images in western Crimea. (a) Original Spot panchromatic scene.

4.1. Reconstructing local stress tensors

The inverse method used provides access to the orientation of the three principal stress axes σ_1 , σ_2 and σ_3 , with $\sigma_1 \geq \sigma_2 \geq \sigma_3$ (pressure positive), and to the value of the ratio Φ defined as $\Phi = (\sigma_2 - \sigma_3) / (\sigma_1 - \sigma_3)$, ($0 \leq \Phi \leq 1$), related to the shape of the stress ellipsoid (oblate for $\Phi > 0.5$, prolate for $\Phi < 0.5$). Using the inverse method allows calculation of the reduced stress tensor ('R4DT' method, Angelier, 1984; 'INVD' method, Angelier, 1984, 1990).

Most studied sites were affected by a polyphase tectonic history, so that the measured faults have been created or reactivated under several successive palaeostress regimes. It was thus necessary to split sets of data into two or more mechanically homoge-

neous subsets (e.g., Fig. 11a, simple example with two subsets). Reactivation of fault planes with successive slip indicated by various striae are common (e.g., Fig. 11b). We could often establish the chronology of stress tensors by considering the tilting of layers related to a known folding event, considering that one of the three principal stress axes was nearly vertical when faulting occurred, as observed in untilted sites (e.g., Fig. 11c). We thus distinguished pre-tilt, syn-tilt and post-tilt stress regimes.

4.2. Tectonic behaviour of large structures

Analysis of remote sensing data allowed us to identify the largest structures in Crimea, and their tectonic behaviour was constrained by inversion of fault slip data. This approach resembles that already

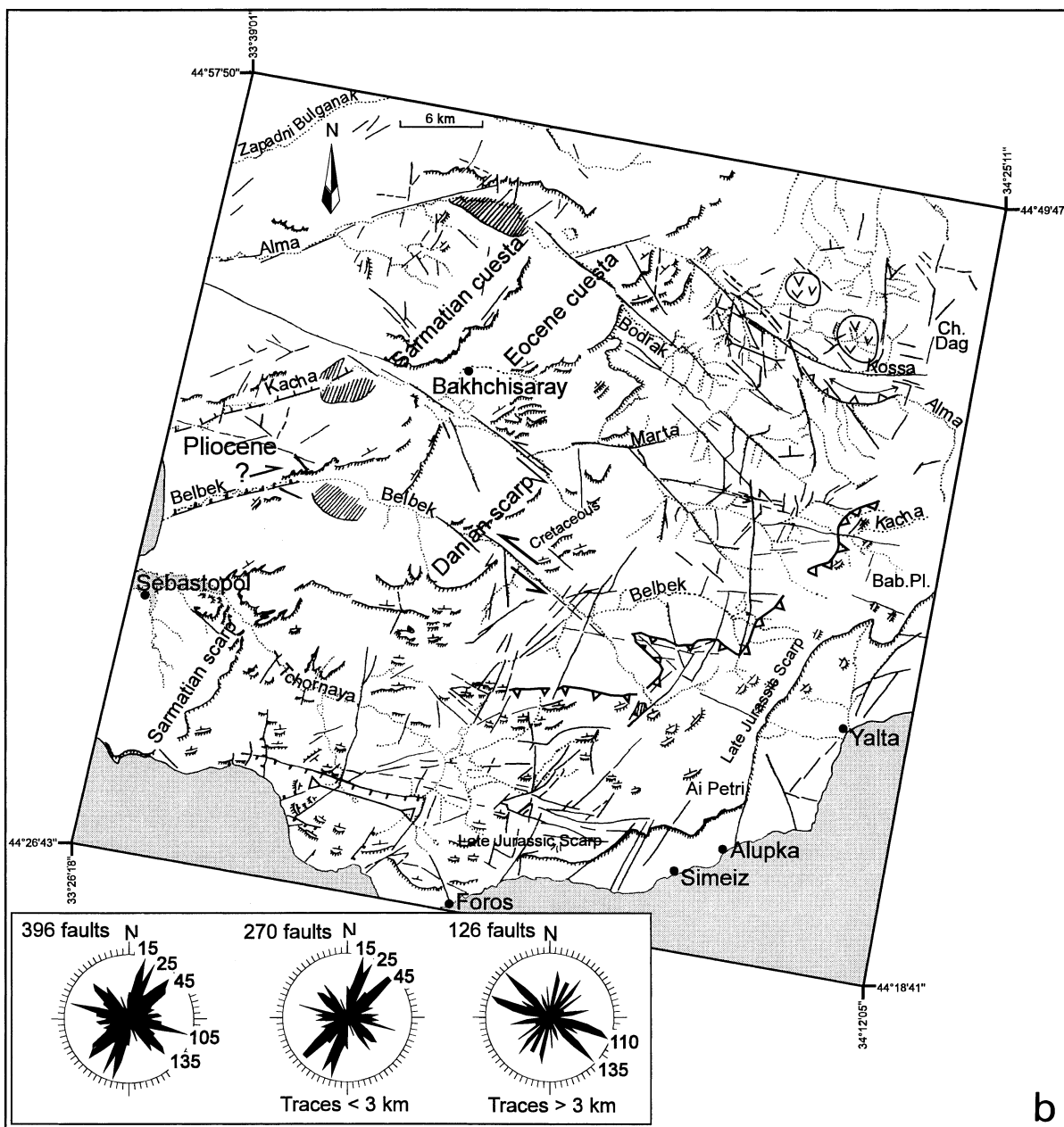


Fig. 7 (continued). (b) Corresponding structural map from analyses of Spot panchromatic–Landsat TM couples of western Crimea. Trend distribution of traces added in rose diagram (complete set on the left, subsets with a length boundary of 3 km on the right). *Ba. Pl.* = Babugan Plateau; *Ch. Dag* = Chatyr Dag Massif.

involved in earlier studies of other regions (Chorowicz et al., 1994b). In this sub-section, we discuss the largest structures of western Crimea and eastern Crimea successively, because of the differences

in trends and mechanisms. These differences are highlighted by contrasting strikes of faults that we observed in the field (rose diagrams, Fig. 12).

Large extensional features play an important role



Fig. 8. Local interpretation of Spot image: northwestern slope of the Crimean chain. (a) Spot image.

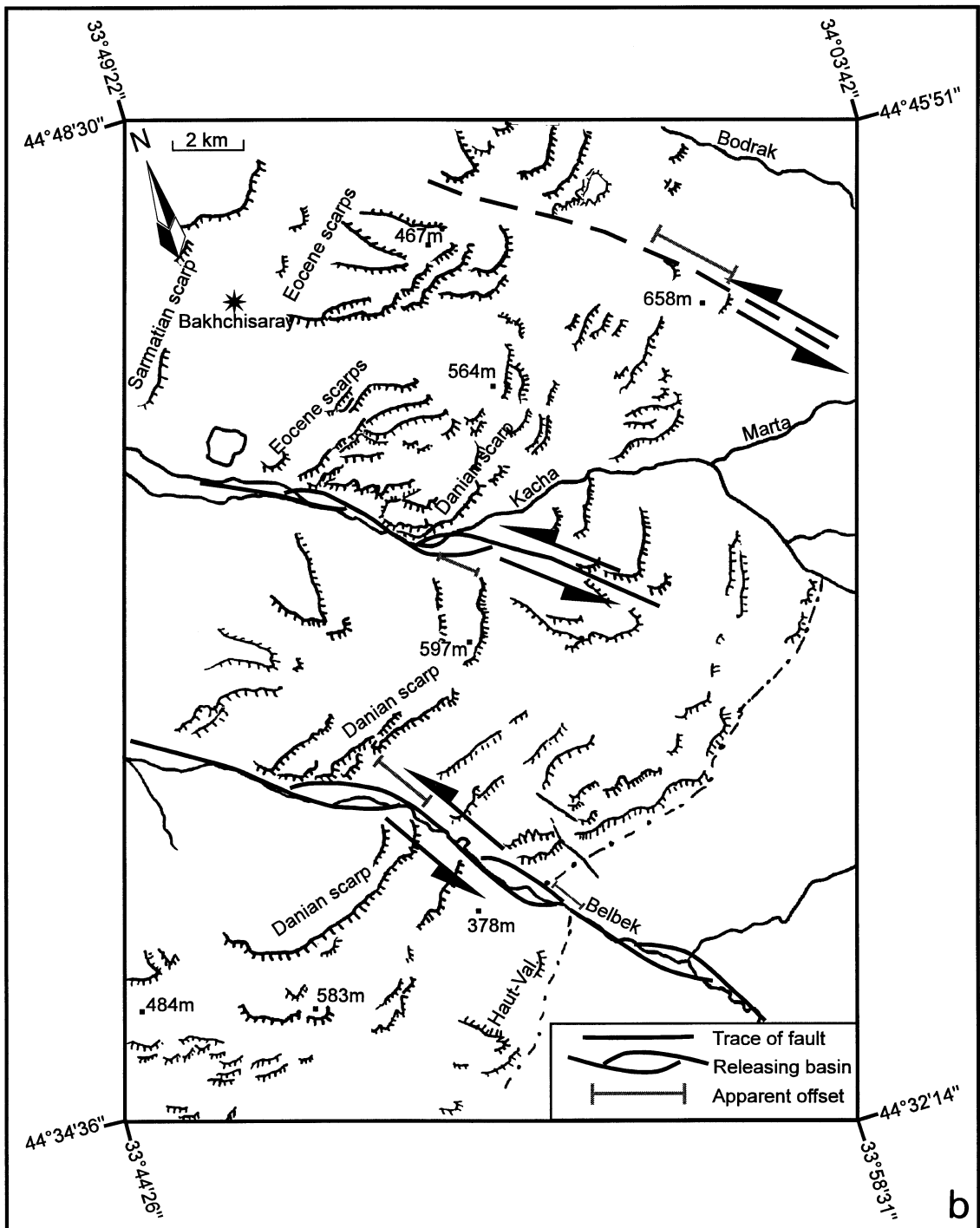


Fig. 8 (continued). (b) Corresponding structural map. Note the left-lateral offsets of the Danian cuesta. The existence of releasing basins indicates that motion is predominantly strike-slip.



Fig. 9. Scarp of Babugan Plateau. (a) Aerial photograph.

in Crimea. The WSW–ENE (N70) large faults of the downstream Alma, Kacha and Belbek river valleys show vertical offsets of terranes with block tilting towards the north in agreement with an extensional regime that we identified by inversion of fault slip data sets (Fig. 13). Contrarily, the senses of displacement along numerous N15, N25, N45 striking faults in western Crimea were not well constrained by remote sensing analyses. Stress tensor determination suggests that these N15- to N70-directed faults underwent a NW–SE extensional regime (Fig. 13).

Numerous tension gashes and isolated normal faults (Fig. 13) belong to this extensional event. This extension fits well with the Oligocene development of the Alma and Sorokin troughs which bordered the Crimea chain (Fig. 13). In this case, the normal faulting in the downstream Alma, Kacha and Belbek river valleys, which affected Pliocene terranes with block-tilting towards the north, represents an event which recently reactivated these WSW–ENE discontinuities (for more explanation, see Section 4.3).

As shown by rose diagrams of strikes of micro-

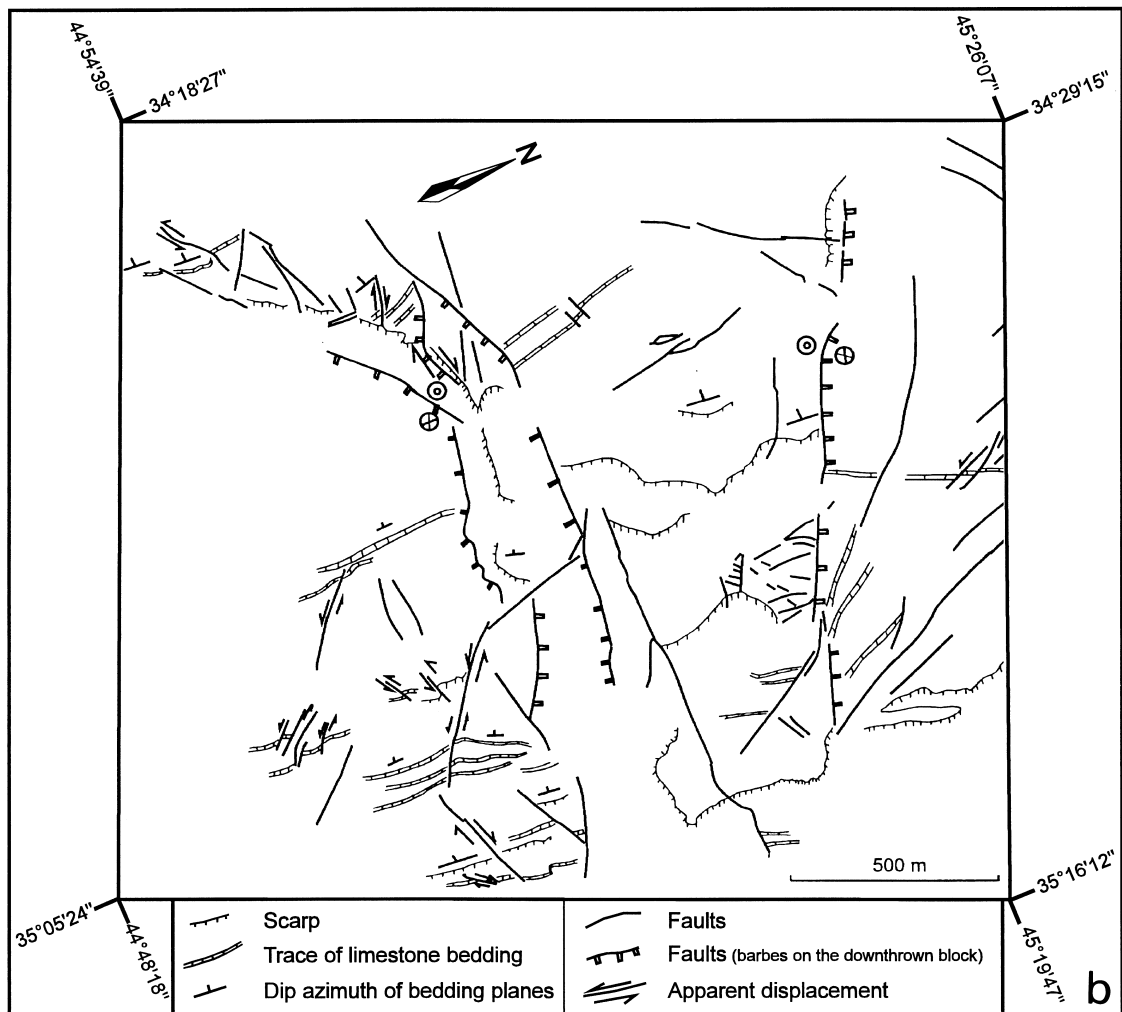


Fig. 9 (continued). (b) Corresponding structural map. Note the presence of normal fault system.

tectonic data that we collected in western Crimea (Fig. 12), the WNW–ESE trend strongly prevails; it is also that of an important population that we detected in the Spot scene (rose diagram in Fig. 7b). The normal displacement along the set of N105–N110 large faults identified in the Spot scene in the southwestern Crimean chain fits well the stress tensors reconstructed in this area (Fig. 14). A good agreement is observed in the vicinity of Foros, between fault strike (rose diagram in Fig. 14) and normal faulting behaviour at microtectonic and the Spot scene scales.

Analysis of satellite imagery fails to show reactivation of these normal faults, which is revealed by

field studies of fault slip data (Figs. 13 and 14). However, these normal faults were reactivated in a strike-slip regime with σ_1 trending NW–SE (Fig. 14), and in sites 8, 32 and 45, in a strike-slip regime with σ_1 trending ENE–WSW (Figs. 13 and 14). Moreover, the numerous stress tensors determined in western Crimea, particularly near Bakhchisaray, suggest that right-lateral displacement occurred along these N105–N110 trends (Fig. 15). The rose diagram (in Fig. 15) of microtectonic data near Bakhchisaray illustrates the two strikes of faulting related to the strike-slip regime which involved WNW–ESE right-lateral strike-slip faults and conjugate N150 minor faults.



Fig. 10. Local interpretation of Spot image: upstream Alma river basin. (a) Spot image.

Such reactivation of large preexisting normal faults also occurred during the latest Plio–Quaternary tectonic events. In the Bakhchisaray region, we observed in the Spot scene a recent left-lateral offset along the sets of N135-trending large faults (see Fig. 16, Section 4.3); according to field observation, the N45-trending large faults are the corresponding right-lateral faults in a conjugate pattern.

As for the Mesozoic events, large N135-trending faults underwent right-lateral displacement during an old strike-slip regime with σ_1 trending NNW–SSE, in agreement with stress tensors that we determined in terranes of the Lower and Middle Complexes (Fig. 17, Section 4.3). In this stress field, the N15 faults (which are well identified in Spot scenes, see rose diagram in Fig. 7b) could be defined as the conjugate left-lateral strike-slip faults of the N135 fault set (Fig. 17). This direction of compression is in agreement with

the folding and thrusting observed in the Lower Complex in the upstream Alma river valley and with the reverse stress tensors that we reconstructed in the Lower and Middle Complexes (Fig. 17). These deformations seem to be related to a transpressional regime with σ_1 trending NNW–SSE to N–S.

The structure of eastern Crimea is simpler. Along the set of N10-striking faults, we observed vertical displacement which fits the E–W extensional regime that we reconstructed based on microtectonic data inversion (Fig. 16, Section 4.3). In addition, we identified left-lateral displacement along this set of N10 faults and right-lateral displacement along associated N140 faults. This system is in agreement with a strike-slip regime that we reconstructed by tensor calculations (Fig. 16, Section 4.3). In site 79, we could observe the reactivation of the N50 and N140 strike-slip faults in the E–W extensional

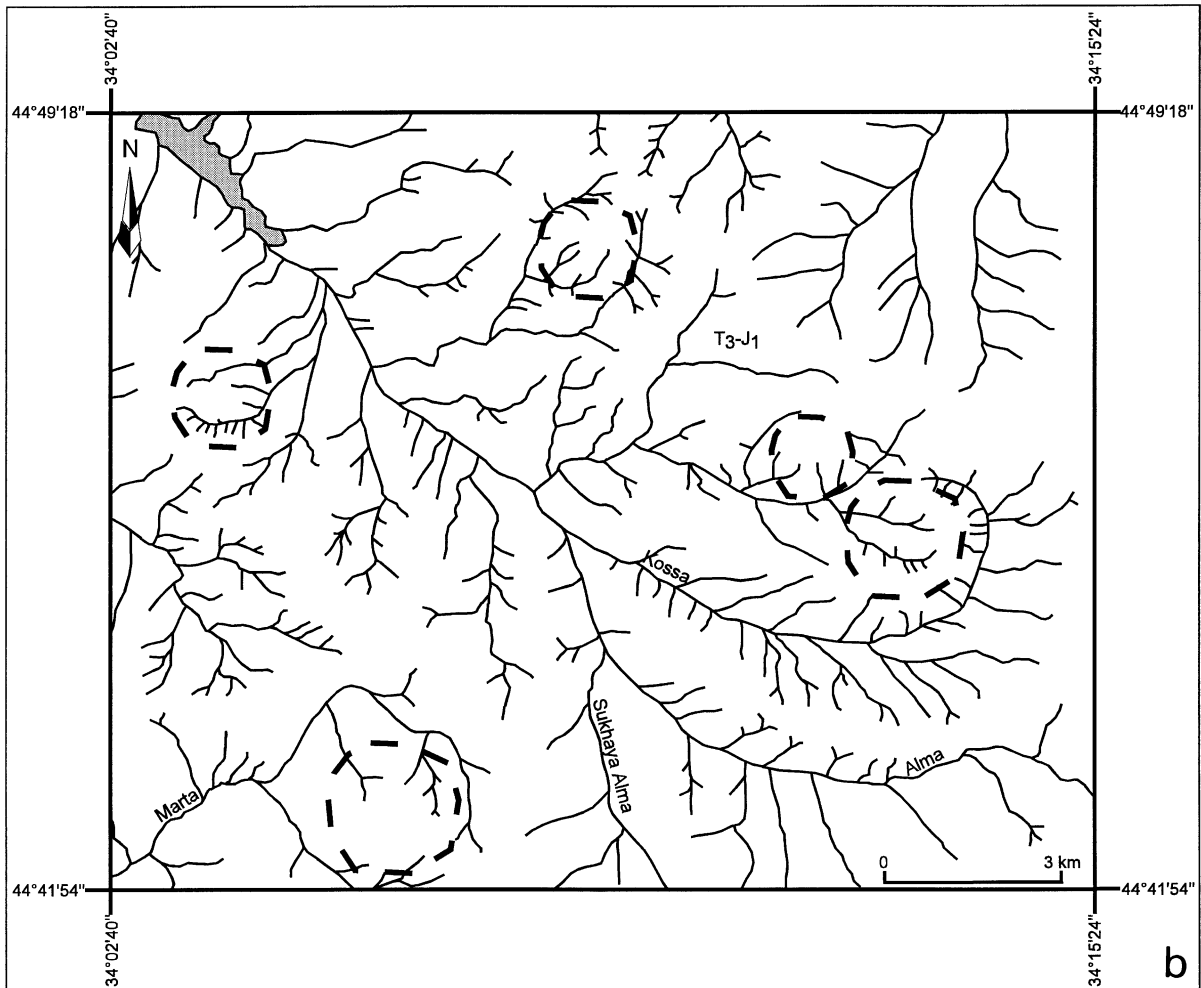


Fig. 10 (continued). (b) Drainage network map. Note the presence of circular drainage anomalies (surrounded by thick dashed lines) revealing probable circular structures at depth.

regime mentioned above; in site 66, the N140 faults suffered reactivation in this extensional regime.

Across the important set of NE–SW (N50) faults that we plotted in the Spot scene of eastern Crimea, we did not observe apparent displacements. Nevertheless, numerous stress tensors allowed us to assume that left-lateral displacement occurred in these fault surfaces in a strike-slip regime with σ_1 trending NNE–SSE (Fig. 17, Section 4.3). This regime seems to be older than the tilting of layers as shown in sites 76 and 81 where the back-tilting tensor was calculated (see diagram in Fig. 17, Section 4.3). It is reasonable to associate with this strike-slip regime

an old reverse regime with σ_1 trending NNE–SSW identified in nearby sites (Fig. 17, Section 4.3). Such a transpressional regime is consistent with the development of the thrusts and folds that we could observe in the Lower and Middle Complexes.

These studies show that the palaeostress analysis allows to constrain the tectonic behaviour of large structures, and that, in turn, the identification of these major structures allows to determine the amplitude of the tectonic regimes. Combining these approaches enables one to identify the tectonic events responsible for the major deformations of the belt. We thus recognised several major regimes in western Crimea:

Table 2
Examples of paleostress results at sites studied in Crimea

Localities	Latitude/Longitude (degrees)	Age of formation	No.	Stress regime	N	σ_1		σ_2		σ_3		Method	ϕ	α	RUP (%)	
						trend	plunge	trend	plunge	trend	plunge					
Bakhchisaray	44.77/33.99	Middle Jur.	1	S	9	180	26	312	54	078	23	INVD	0.1	13	38	
			*	S		003	02	269	60	094	30	INVD	0.1	13	36	
Bakhchisaray	44.77/33.99	Middle Jur.	1	R	14	194	06	103	01	002	84	INVD	0.5	12	22	
Bakhchisaray	44.72/33.85	Palaeogene	2	S	7	100	08	288	82	190	01	INVD	0.6	04	17	
Bakhchisaray	44.72/33.85	Palaeogene	2	S	15	129	01	031	84	220	06	INVD	0.4	11	37	
Bakhchisaray	44.77/33.87	Palaeogene	3	S	25	131	04	294	86	041	01	INVD	0.5	09	29	
Bakhchisaray	44.75/33.85	Late Eoc.	25	S	18	318	08	059	52	222	37	INVD	0.1	12	38	
Bakhchisaray	44.75/33.85	Late Eoc.	25	N	8	127	77	222	01	313	13	INVD	0.3	04	11	
Bakhchisaray	44.75/33.85	Late Eoc.	25	N	9	109	75	286	15	016	01	INVD	0.4	09	24	
Bakhchisaray	44.80/34.00	Middle Jur.	41	R	19	190	09	100	01	006	81	INVD	0.6	11	22	
Bakhchisaray	44.80/34.00	Middle Jur.	41	S	14	171	20	345	70	080	02	INVD	0.4	11	25	
Bakhchisaray	44.80/34.00	Middle Jur.	41	S	8	112	10	224	65	018	22	INVD	0.5	14	35	
Bakhchisaray	44.80/34.00	Middle Jur.	41	S	6	340	46	131	40	234	15	INVD	0.7	09	28	
Simferopol	44.95/34.17	Middle Jur.	32	N	18	317	79	217	02	127	11	INVD	0.5	10	24	
Simferopol	44.95/34.17	Middle Jur.	32	S	17	074	01	339	77	164	13	INVD	0.4	12	34	
Simferopol	44.95/34.17	Middle Jur.	32	S	9	178	21	311	60	080	20	INVD	0.6	05	26	
Belogorsk	45.07/34.67	Middle Eoc.	30	N	18	297	82	177	04	087	07	INVD	0.3	10	27	
Belogorsk	44.97/34.63	Tithonian	63	S	14	164	01	066	80	254	10	INVD	0.4	16	34	
Belogorsk	44.97/34.63	Tithonian	63	S	17	008	14	142	70	274	13	INVD	0.4	13	28	
Belogorsk	45.05/34.60	Eocene	84	S	5	327	46	141	44	234	03	R4DT	0.8	01		
Staryi Krym	44.97/34.98	Tithonian	76	S	12	208	50	048	39	310	10	INVD	0.3	11	37	
			*	S		12	027	06	125	51	292	38	INVD	0.2	12	40
Staryi Krym	44.97/34.98	Tithonian	76	S	21	359	13	258	41	103	47	INVD	0.3	08	22	
Staryi Krym	45.00/35.07	Tithonian	79	N	14	309	72	195	08	103	16	INVD	0.5	09	34	
Staryi Krym	45.00/35.07	Tithonian	79	S	15	338	17	212	63	075	21	INVD	0.4	12	34	
Staryi Krym	45.00/35.07	Tithonian	79	S	18	014	07	258	74	106	15	INVD	0.5	10	26	
Foros	44.41/33.70	Late Jur.	8	N	43	175	77	270	01	360	13	INVD	0.4	12	29	
Foros	44.41/33.70	Late Jur.	8	S	6	247	21	103	65	343	13	INVD	0.5	08	36	
Foros	44.37/33.68	Oxfordian	9	S	13	142	42	322	48	052	00	INVD	0.6	11	36	
Foros	44.37/33.68	Oxfordian	47	S	30	304	15	178	66	039	19	R4DT	0.2	12		
Foros	44.48/33.88	Oxfordian	48	N	7	130	83	270	05	001	04	INVD	0.3	12	33	
Yalta	44.40/34.07	Oxfordian	45	R	20	336	01	245	60	066	30	R4DT	0.1	13		
Yalta	44.40/34.07	Oxfordian	45	N	9	283	80	044	05	134	09	INVD	0.3	07	17	
Yalta	44.40/34.07	Oxfordian	45	N	18	340	81	090	03	180	08	INVD	0.5	09	26	
Yalta	44.40/34.07	Oxfordian	45	S	15	252	15	064	75	161	02	INVD	0.6	19	35	
Yalta	44.57/34.07	Taurian	50	N	9	023	78	215	12	124	02	INVD	0.5	06	24	
Yalta	44.52/34.22	Taurian	52	S	8	112	02	005	83	203	06	INVD	0.6	13	39	
Yalta	44.52/33.98	Oxfordian	59	S	6	348	09	148	80	257	03	INVD	0.6	06	15	
Alushta	44.62/34.32	Middle Jur.	53	S	8	180	15	000	75	090	00	INVD	0.4	08	21	
Sudak	44.80/34.94	Oxfordian	5	R	8	182	21	273	04	015	69	INVD	0.2	12	30	
Sudak	44.86/35.07	Oxfordian	11	R	13	218	04	128	04	351	84	INVD	0.6	10	25	
Sudak	44.87/34.63	Neocomian	61	S	8	347	32	171	58	078	02	INVD	0.7	04	13	
Sudak	44.85/35.08	Late Jur.	64	S	14	172	18	047	61	270	22	INVD	0.5	15	34	
Sudak	44.85/35.08	Late Jur.	64	N	7	129	70	006	12	273	17	INVD	0.4	08	25	
Sudak	44.84/35.08	Late Jur.	65	S	6	330	64	152	26	062	01	INVD	0.7	07	25	
Sudak	44.86/35.08	Late Jur.	66	N	21	293	84	151	05	061	03	INVD	0.1	18	57	
Sudak	44.90/35.13	Late Jur.	67	N	4	201	74	028	16	297	02	INVD	0.6	07	22	
Feodosya	44.93/35.18	Middle Jur.	68	R	20	213	06	303	01	039	84	INVD	0.5	14	34	
Feodosya	44.95/35.27	Late Jur.	81	S	21	018	22	156	61	281	17	INVD	0.6	09	28	
			*	S		21	017	01	111	75	287	15	INVD	0.6	09	28
Kertch	45.32/36.34	Neogene	12	R	19	124	08	033	02	290	82	INVD	0.5	11	39	

Table 2 (continued)

Localities	Latitude/Longitude (degrees)	Age of formation	No.	Stress regime	<i>N</i>	σ_1		σ_2		σ_3		Method	Φ	α	RUP (%)
						trend	plunge	trend	plunge	trend	plunge				
Kertch	45.32/36.34	Neogene	12	R	16	160	11	251	05	004	78	INVD	0.5	08	30
Kertch	45.32/35.67	Late Mioc.	70	N	4	028	58	181	29	278	12	INVD	0.7	10	26
Kertch	45.40/35.73	Late Mioc.	71	N	21	214	83	001	06	091	04	INVD	0.3	10	30
Kertch	45.15/36.42	Late Mioc.	128	R	17	319	02	049	01	182	88	INVD	0.6	04	11
Kertch	45.42/36.55	Mid. Mioc.	130	R	36	132	08	042	01	304	82	INVD	0.4	10	31

No., reference number of the site. Stress regimes: S, strike-slip faulting; R, reverse faulting; N, normal faulting. *N*, number of fault slip data. Trends and plunges of stress axes in degrees (with * for backtilted stress tensors). Methods (INVD and R4DT) referred to in Angelier (1990). Φ , ratio of stress magnitude differences, $\Phi = (\sigma_2 - \sigma_3)/(\sigma_1 - \sigma_3)$. α , average angle between observed slip and computed shear, in degrees (acceptable with $\alpha < 22.5^\circ$). RUP, criterion of quality for the 'INVD' method, ranging from 0% (calculated shear stress parallel to actual striae with the same sense and maximum shear stress) to 200% (calculated shear stress maximum, parallel to actual striae but opposite in sense), acceptable results with RUP < 75%.

(1) a transpressional regime with σ_1 trending N–S to NNW–SSE probably responsible for the development of strike-slip faults (striking N15 and N135), reverse faults and large folds and thrusts in the Lower and Middle Complexes, and that we assigned to the late Cimmerian phase; (2) a N–S extension which affected the Eocene rocks (site 25); (3) a NW–SE extension that we interpreted to be related to the development of peripheral troughs in Oligocene times and which developed normal faulting along N15, N25, N50, N70 strikes; (4) the latest strike-slip regime with σ_3 trending NNE–SSW which reactivated the N135 faults in a well observed left-lateral displacement. Other regimes (strike-slip regime with σ_1 trending NW–SE and strike-slip regime with σ_1 trending NE–SW) were also identified in the field but do not correspond to major features observable in the images. In eastern Crimea, we identified two major regimes of deformation which fit well with the two palaeostress fields that we determined: (1) an old NNE–SSW transpressional event which developed strike-slip faults, folds and thrusts affecting Lower and Middle Complexes, and (2) a recent transtensional regime with σ_3 trending E–W, responsible of the well observed latest strike-slip and normal faulting. Both are related to major structures.

4.3. Remote sensing, palaeostress analysis and recent tectonism

Fig. 16 illustrates the neotectonics scheme of Crimea including the latest deformation and as-

sociated stress field. We attempt to explain the fan-shaped distribution of the latest active faults which strike NNE–SSW, NE–SW, NW–SE in eastern Crimea and WNW–ESE, NW–SE, ENE–WSW in western Crimea. We have to take into account the associated faulting modes (normal and strike-slip). We noticed the good fit between NNE–SSW microtectonic data sets that we collected near Belogorsk (rose diagram in Fig. 16) and the attitude of the largest discontinuities of eastern Crimea. In the vicinity of Partenit, the strikes of microtectonic data sets are WSW–ESE and NW–SE (rose diagram in Fig. 16) like those of the largest structures developed in western Crimea. The latest deformation fits well with both the fan-shaped recent stress field recognised through field analyses (Saintot et al., 1998) and the inversion of focal mechanisms (Goushtchenko et al., 1993). The maximum principal stress axis σ_1 trends NNW–SSE in eastern Crimea and WNW–ESE in western Crimea (Fig. 16). One may think that the arcuate shape of the Crimean belt results from the oblique collision of the East Black Sea Plate following a NNW direction of convergence, the East Black Sea Plate acting as an indenter. In eastern Crimea, the reverse regime with σ_1 trending NNW–SSE prevailed offshore and in the Kertch Peninsula. Numerous folds and reverse faults were observed in the Kertch Peninsula, in agreement with the NNW–SSE direction of compression (Fig. 16). In this context, the Crimean Mountains underwent an uplift, so that the stress regime changed to a strike-slip regime. This stress field is in agreement with the NNE–SSW

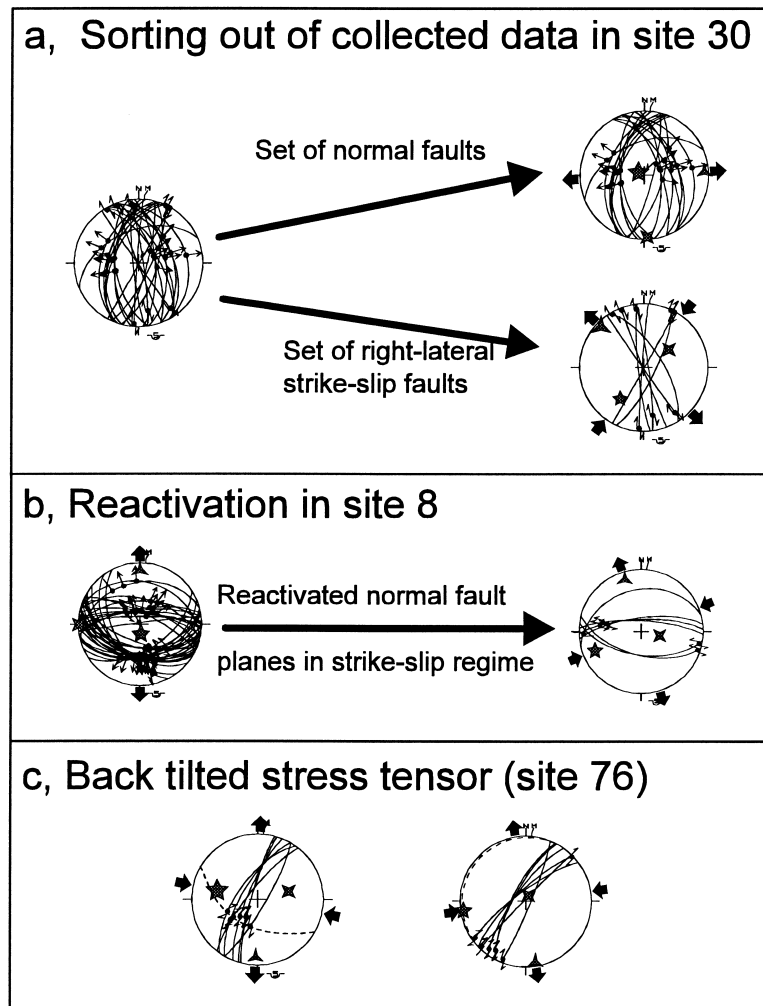


Fig. 11. Examples of polyphase tectonism. (a) Fault population collected in site 30, near Belogorsk. The whole set is divided into two subsets, consistent with different stress regimes. Stereoplot: Schmidt's projection, lower hemisphere. Bedding planes as broken lines, fault planes as thin lines, striae as small arrows (inward directed = reverse, outward directed = normal, couple of thin arrows = strike-slip). Computed stress axes as 5-, 4- and 3- branch stars (σ_1 , σ_2 and σ_3 , respectively). Direction of compression: inward-directed arrows; direction of extension: outward-directed arrows. (b) Normal fault reactivated in a strike-slip regime, as shown by superposed sets of striae; site 8 near Foros. (c) Backtilted stress tensor, site 76, near Saryi-Krym.

left-lateral strike-slip faults and the NW–SE right-lateral strike-slip faults in eastern Crimea, and with the NW–SE left-lateral strike-slip faults and the NE–SW right-lateral strike-slip faults in western Crimea. The northern flank of Crimea is characterised by extensional deformation along nearly WSW–ENE faults in the western Crimean foreland and nearly N–S faults in the eastern Crimean foreland. In the frame of our conception of the geodynamic con-

text, the Cenozoic terranes of the foreland suffered stretching, with a trend of extension perpendicular to the trend of compression. Tension gashes measured in Mio–Pliocene terranes of the western foreland (Fig. 16) are in good agreement with a probable extensional regime which recently prevailed in this region. In the Eocene formations of the foreland of eastern Crimea as well as in the northwestern part of the Kertch Peninsula, we observed that the N10

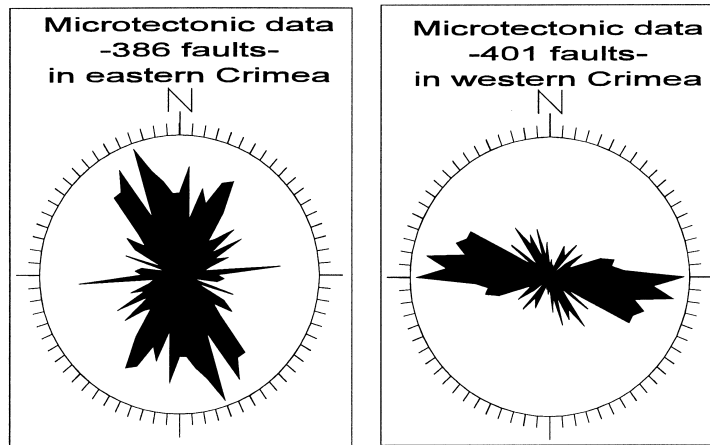


Fig. 12. Rose diagrams of strikes, minor faults data collected in the field in eastern and western Crimea. Compare with rose diagrams in Fig. 3b and Fig. 7b, respectively.

striking sets of large faults underwent nearly E–W extension in agreement with the brittle microtectonic data and reconstructed stress tensors (Fig. 16). We noticed in the core of the eastern Crimean chain local E–W extension related to the more general strike-slip regime, with σ_3 trending E–W; we explain this pattern by local permutations of the σ_1 and σ_2 principal stress axes.

To summarise our model for Plio–Quaternary times, onshore Crimea underwent deformations in a strike-slip regime in the core of the chain (clear transtensional regime in eastern Crimea) and in an extensional regime in the foreland, with an obvious fan-shaped distribution of tectonic stresses and faults.

4.4. How far can old events be reconstructed?

Combined mechanical and geometric analyses in the Lower and Middle Complexes allowed us to determine ancient tectonic events. We identified a characteristic structural pattern in the older terranes of Crimea (the Lower Complex) which corresponds to a N–S south-vergent compression. The structure of the allochthonous Middle Complex is complicated by internal thrusting (as for the two units in tectonic contact seen at the bottom of the Dolgoruki Plateau), in agreement with a NNE–SSW compression. This nearly N–S compressional event is not recorded in the Upper Complex of Crimea. The de-

termination of tectonic stress tensors which affected the Lower and Middle Complexes in western Crimea indicates that the trend of compression was N–S and NNW–SSE whereas it was NNE–SSW in eastern Crimea (Fig. 17). The reconstructed stress tensors are compressional or strike-slip as well, indicating that Crimea underwent a transpressional regime during the latest Cimmerian phase. This early stress field was not consistent throughout the belt: a deviation existed in the trend of compression, from NNE–SSW in eastern Crimea to N–S and NNW–SSE in western Crimea.

In a region where polyphase tectonism occurs, the reactivation of structures may overprint the record of old tectonism. This study has shown that it is however possible to obtain information on the mechanisms of the early structural development of Crimea, because the old events left strong marks in terms of deformation, which were not all overprinted by recent reactivation.

5. Conclusions

The remote sensing analysis provides a general account of the geometry of large structures. Particular attention was paid to the orientations of mechanical discontinuities because of their potential for reactivation under later stress regimes. The approach in terms of conjugate fault patterns is efficient as

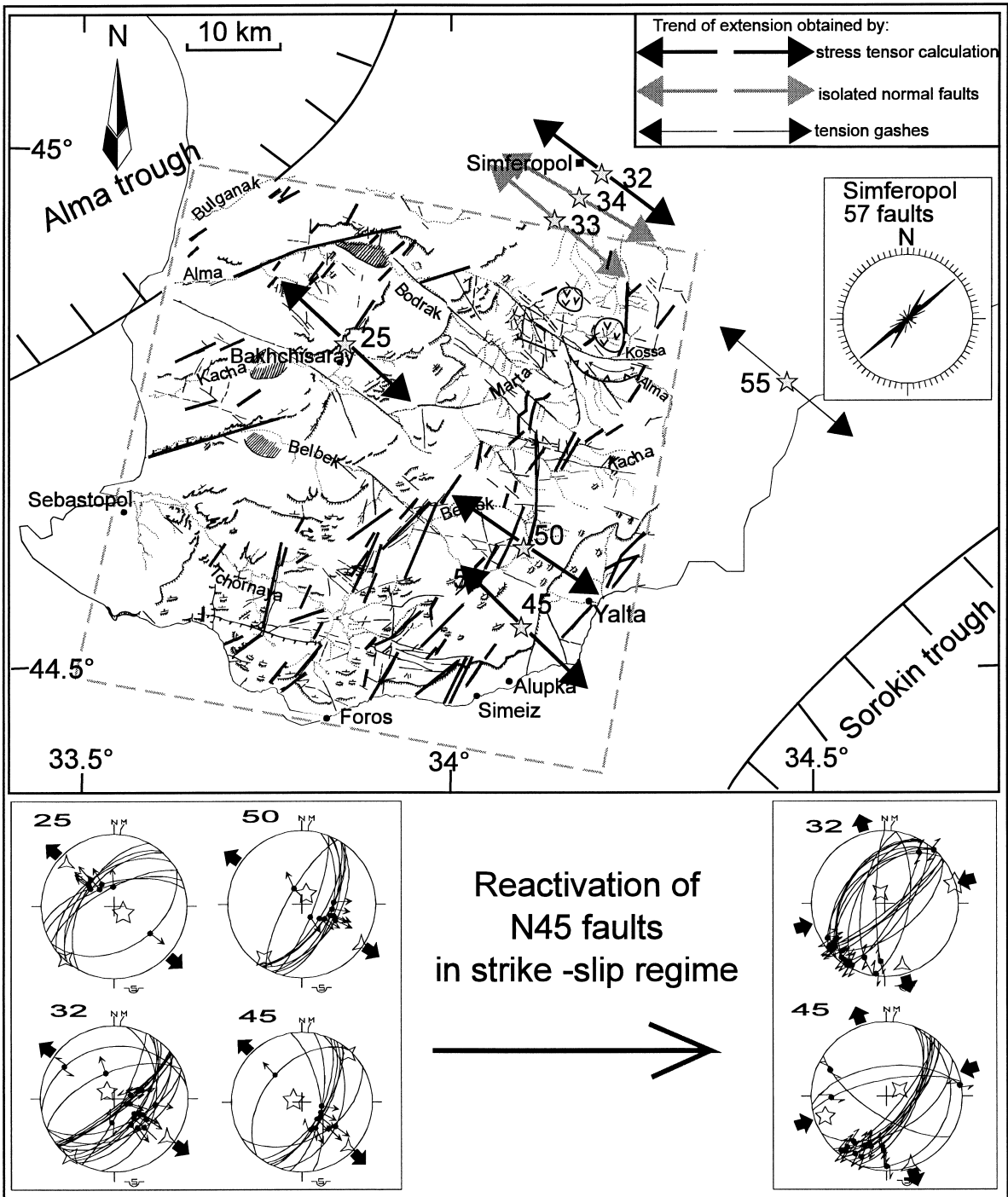


Fig. 13. Structural pattern and local palaeostress tensors related to NW–SE extensional event in western Crimea. Large faults involved in this regime as thick lines; explanation of stereoplots as for Fig. 11a; sites located in map as grey stars with reference number.

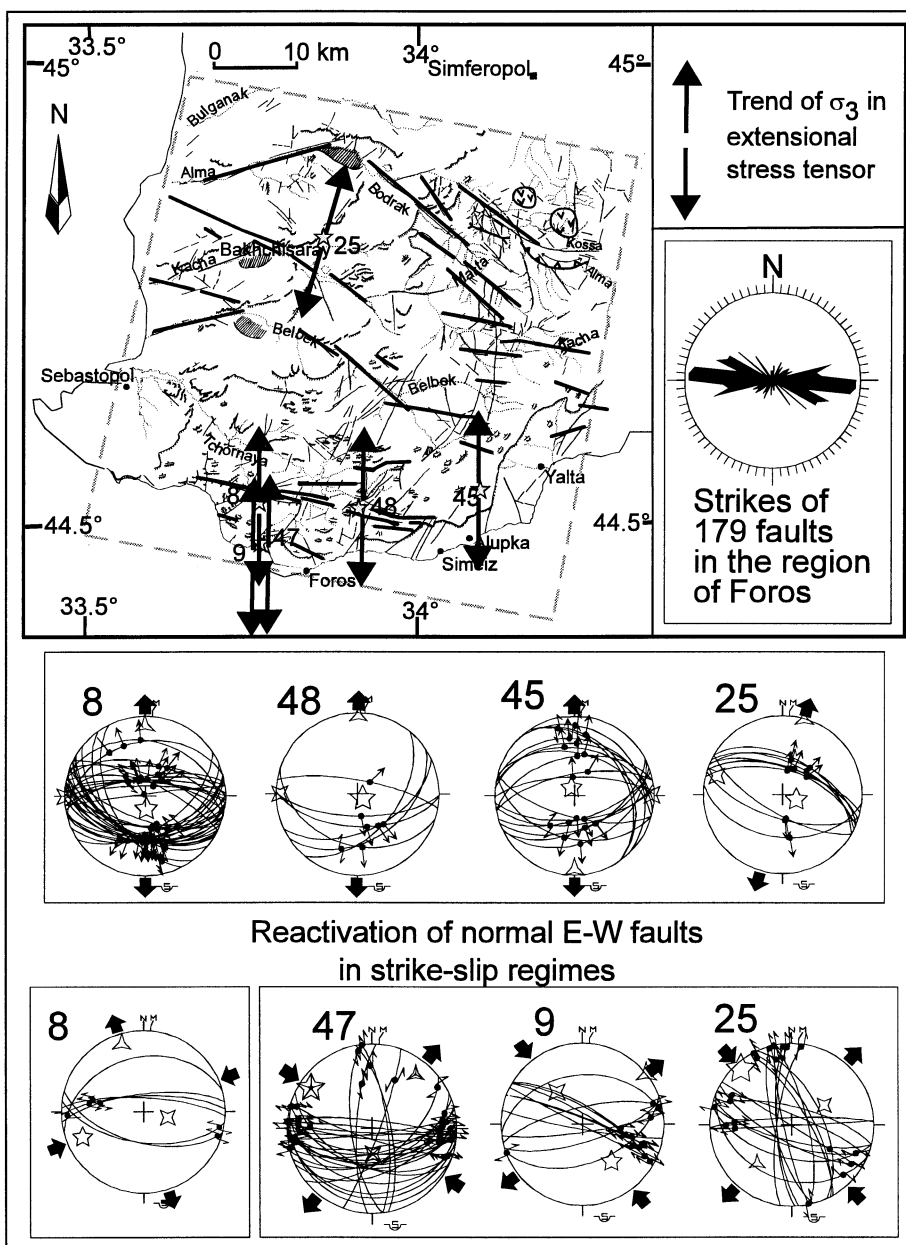


Fig. 14. Structural pattern and local palaeostress tensors related to N–S extensional event in western Crimea. Explanation as for Fig. 13.

far as newly formed brittle structures are concerned. Mechanical analysis of brittle tectonics in the field is compulsory, because it enables one to reconstruct and interpret reactivation of discontinuities under successive palaeostresses, which results in oblique slips that can hardly be detected in the images.

However, we note that, close to the major faults, the minor fault-fracture patterns often correspond to simple conjugate systems which are mechanically consistent with the reactivation of the main fault.

We thus identified major tectonic events that have affected Crimea since Berriasian times:

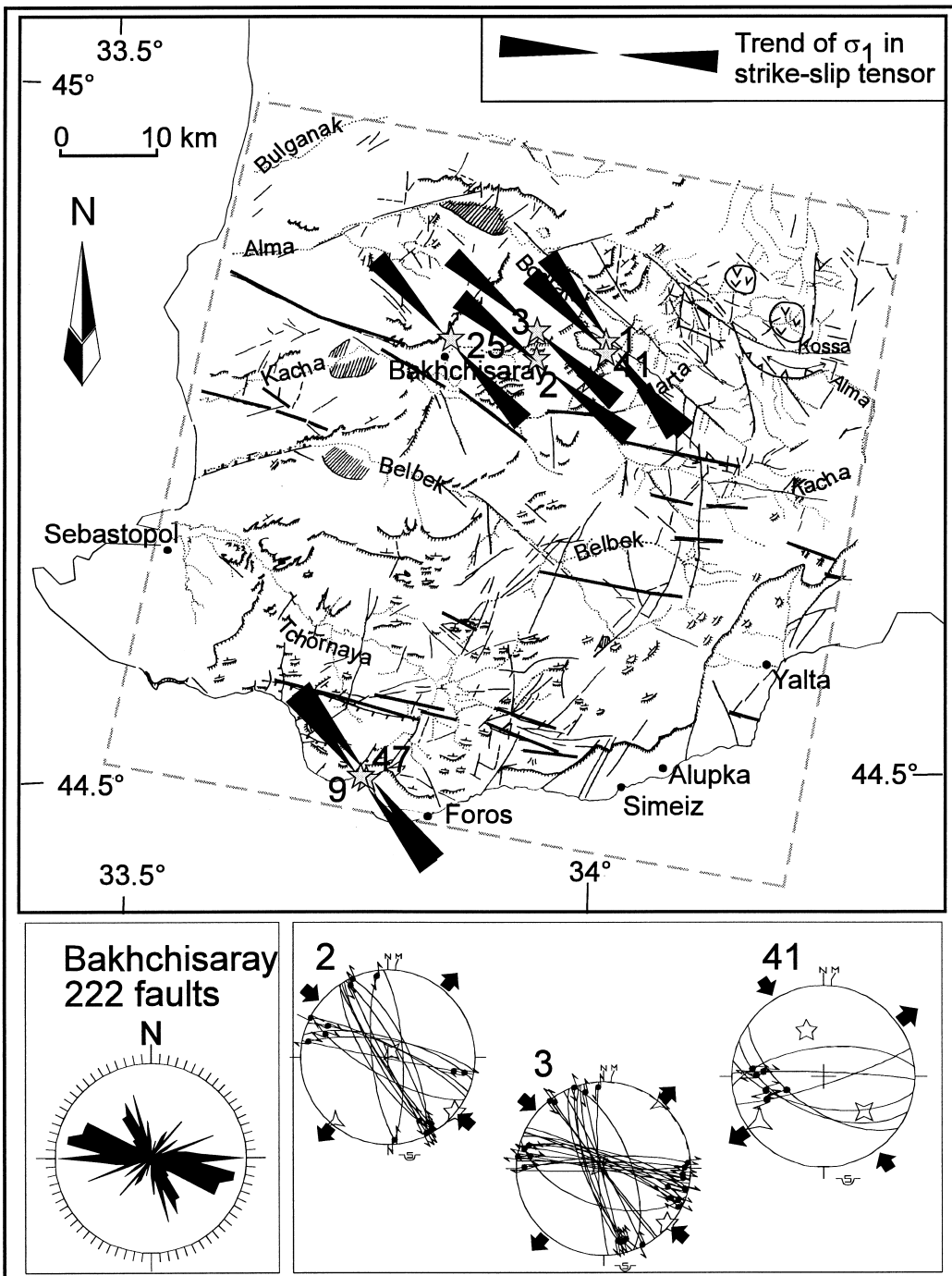


Fig. 15. Structural pattern and local palaeostress tensors related to strike-slip regime in western Crimea, with σ_1 trending NW–SE. Explanation as for Fig. 13.

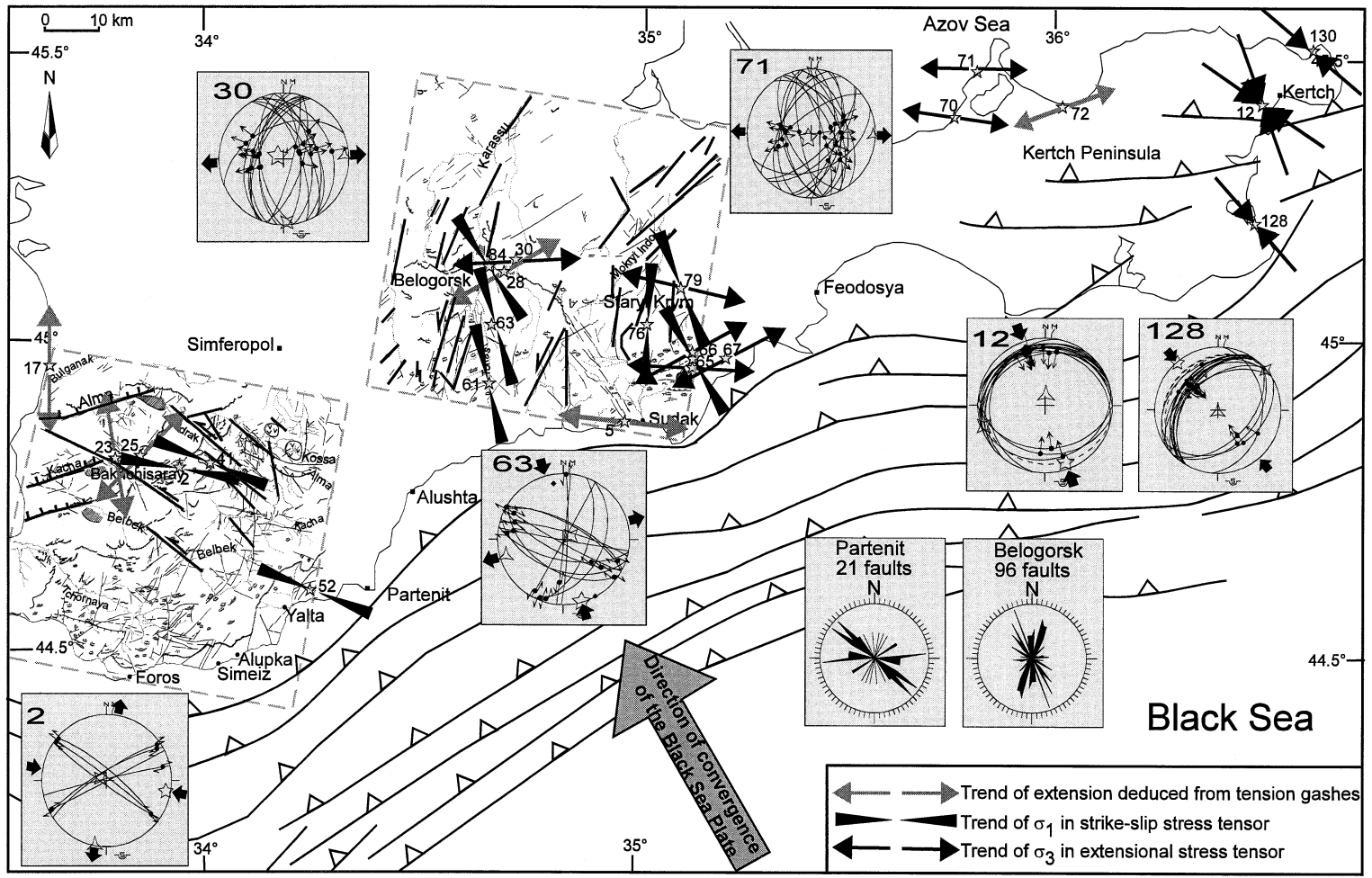


Fig. 16. Neotectonics of Crimea. Explanation as for Fig. 13.

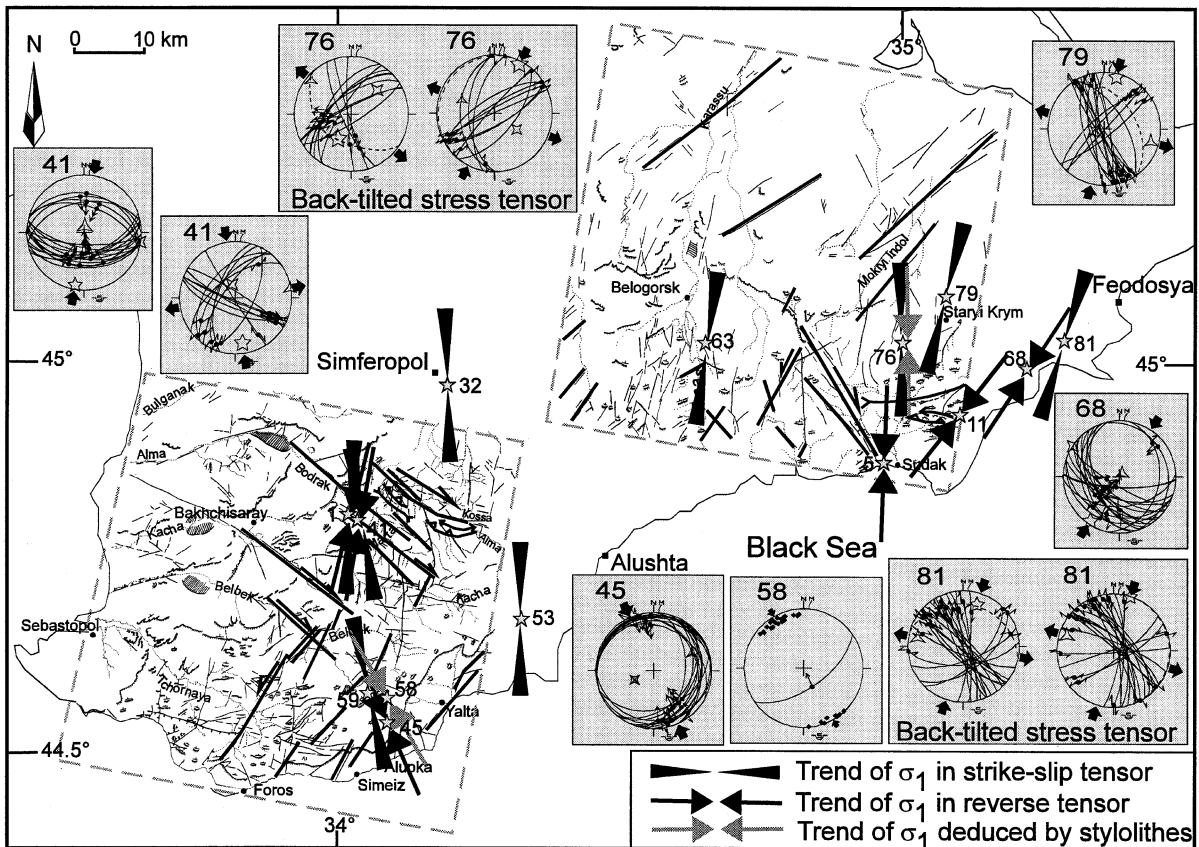


Fig. 17. Summary of structural features in Spot scenes and palaeostress local tensor related to thrusting and folding of the compressional event of the late Cimmerian phase. Explanation as for Fig. 13.

(1) A transpressional regime, with σ_1 trending N–S to NNW–SSE in western Crimea and NNE–SSW in eastern Crimea, which characterised the late Cimmerian phase.

(2) A N–S extension and a NW–SE extension restricted to western Crimea, and related to the development of peripheral troughs in Oligocene times; because of the general perpendicularity between extension and trough trends, deviatoric stresses related to deep trough development may have played a major role.

(3) The latest regime is transtensional onshore, with σ_3 trending NNE–SSW in western Crimea. The NW–SE faults were reactivated as left-lateral, with σ_3 trending E–W in eastern Crimea, responsible of the widespread strike-slip and normal faulting that occurred latest.

We finally point out that the tectonics in Crimea were heterogeneous, a phenomenon that may be explained by the presence of the major deep NW–SE Alushta–Simferopol fault, as an important discontinuity controlling the difference of behaviour of the eastern and western parts of the Crimean Mountains.

Acknowledgements

The Peri-Tethys Programme and M.E.S.R. for financial supports; I.S.I.S. committee for the acceptance of our project, A. Ilyin who allowed to us to carry out field trips, M. Nikitin for providing aerial photographs, B. Deffontaines for help in remote sensing analysis; A.M. Nikishin and an anonymous referee for helpful comments.

References

- Adamia, Sh.A., Gamkrelidze, I.P., Zakaradzie, G.S., Lordkipanidze, M.B., 1977. Adzharo-Trialetsky progib i problema formirovaniya glubokovodnoi vpadiny Chernogo morya (Adzharo-Trialetian depression and problem of formation of deep basin of the Black Sea). *Geotectonika* 1, 78–94.
- Angelier, J., 1984. Tectonic analysis of fault slip data sets. *J. Geophys. Res.* 89 (B7), 5835–5848.
- Angelier, J., 1990. Inversion of field data in fault tectonics to obtain the regional stress, III. A new rapid direct inversion method by analytical means. *Geophys. J. Int.* 103, 363–376.
- Angelier, J., Goushtchenko, O.I., Saintot, A., Ilyin, A., Rebetsky, Y., Vassiliev, N., Yakovlev, F., Malutin, S., 1994. Relations entre champs de contraintes et déformations le long d'une chaîne compressive-décrochante: Crimée et Caucase (Russie et Ukraine). *C.R. Acad. Sci. Paris* 319, Sér. II, 341–348.
- Arkhipov, I.V., Uspenskaya, Ye.A., 1967. Geological Map of Crimea, 1/1,000,000 (in Russian). In: Muratov, M.V. (Ed.), *Geology of U.S.S.R. Ministry of Geology USSR*.
- Boccaletti, M., Gocev, P., Manetti, P., 1974. Mesozoic isotopic zones in the Black Sea region. *Soc. Geol. Ital. Boll.* 93, 547–565.
- Boccaletti, M., Cassinis, R., Dainelli, P., Marino, C.M., Tibaldi, A., Zanchi, A., 1988. Landsat features in the Black Sea area: their tectonic significance. In: *Monograph of the Black Sea. Boll. Geofis. Teor. Appl.* 30 (117–118), 17–38.
- Byzova, S.L., 1980. Netokorye voprosy tektoniki Gornogo Kryma (Some questions of the tectonic of the Crimean Mountains). *Vestn. Mosk. Univ.* 4 (6), 15–25.
- Byzova, S.L., 1981. Suschestvovalo li podnyatie na meste Gornogo Kryma v rannem melu (Was there an uplift on the site of the Crimean Mountains in the Early Cretaceous?) *Bull. MOIP. Otd. Geol.* 56 (1), 41–51.
- Chorowicz, J., Luxey, P., Lyberis, N., Carvalho, J., Parrot, J.F., Yürür, T., Gündogdu, N., 1994a. The Maras Triple Junction (Southern Turkey) based on digital elevation model and satellite imagery interpretation. *J. Geophys. Res.* 99 (B10, 20), 225–242.
- Chorowicz, J., Collet, B., Bonavia, F., Tesfaye, K., 1994b. NW to NNW extension direction in the Ethiopian Rift deduced from the orientation of structures and fault slip analysis. *Geol. Soc. Am., Bull.* 105, 1560–1570.
- Chorowicz, J., Luxey, P., Yürür, T., Rudant, J.P., Gündogdu, N., Lyberis, N., 1995. Slip motion estimation along the Ovacik Fault near Erzincan (Turkey) using ERS-1 radar images. *Remote Sensing Environ.* 52, 66–70.
- Deffontaines, B., Chorowicz, J., 1991. Principles of drainage basin analysis from multisource data: application to the structural analysis of the Zaire Basin. In: Fourniquet, J., Pierre, G. (Eds.), *Neotectonics. Tectonophysics* 194, 237–263.
- Derenyuk, N.E., Vanina, M.V., Gerasimov, M.Ye., Pirovarov, S.V., 1984. Geological map of the Crimea (in Russian). Geological Ministry of Ukraine, Kiev, 1/200,000.
- Doushevsky, V.P., Lysenko, N.I., 1978. Vozrast razryvnykh narusheniy Vostotchno-Krymskogo predgoriya (The age of faults in the Eastern pre-mountain part of Crimea). *Bul. MOIP. Otd. Geol.* 1, 51–53.
- Finetti, I., Bricchi, G., Del Ben, A., Pipan, M., Xuan, Z., 1988. Geophysical study of the Black Sea. In: *Monograph of the Black Sea. Boll. Geofis. Teor. Appl.* 30 (117–118), 197–324.
- Galkin, V.A., Fëdorov, Ye.V., Bakhor, K., 1994. The Interrelationships and Structure of the Upper Jurassic and Lower Cretaceous deposits in the Salgir River Valley (Central Crimea). *Trans. Russian Acad. Sci., Earth Sci. Sect.* 326 (7), 55–60.
- Goushtchenko, O.I., Rebetsky, Y.L., Mikhailova, A.V., Goushtchenko, N.Y., Kuok, L.M., Rassanova, G.V., 1993. The recent regional field of stresses and the mechanism of the lithosphere deformation of seismoactive East-Asia region. *Terra Abstr., Suppl.* 1, Terra Nova 5, 259.
- Kazantsev, Yu.V., 1982. *Tektonika Kryma (Tectonics of the Crimea)*. Nauka, Moscow. 112 pp.
- Kazantsev, Yu.V., Kazantseva, T.G., Arzhavitina, M.Yu., 1989. *Strukturnaya Geologiya Kryma (Structural Geology of the Crimea)*. Ufa, 154 pp.
- Kazmin, V.G., Sbornshikov, I.M., Ricou, L.-E., Zonenshain, L.P., Boulin, J., Knipper, A.L., 1986a. Volcanic belts as markers of the Mesozoic–Cenozoic active margin of Eurasia. *Tectonophysics* 123, 123–152.
- Kazmin, V.G., Ricou, L.-E., Sbornshikov, I.M., 1986b. Structure and evolution of the passive margin of the eastern Tethys. *Tectonophysics* 123, 153–179.
- Khain, V.Ye., 1984. *Regionalnaya geotektonika. Alpiysko-Sredizemnomorskiy poiyas. (Regional geotectonics. The Alpine–Mediterranean Belt)*. Nedra, Moscow, 344 pp.
- Koronovsky, N.V., 1984. The Scythian Plate. In: *Regional Geology of USSR. Moscow State Univ. Press*, pp. 211–212.
- Koronovsky, N.V., Mileev, V.S., 1974. O sootnoshenii otlojenii Tavricheskoi serii i eskiordinkoi svity v doline r. Bodrak (Gornii Krim) (About the relationships of Tauric series and Eskirda suite in the Bodrak river valley (Mountain Crimea)). *Vestn. Mosk. Univ., Geol.* 1, 80–87.
- Kunin, N.Ya., Kosova, S.S., Blokhina, G.Yu., 1989. Recognition of the non-anticline traps for oil and gas based on seismostratigraphic analysis (an example of the eastern Peri-Caucasus region). *VNIIOENG, Moscow*, 43 pp. (in Russian).
- Letouzey, J., 1977. *Synthèse des données géophysiques et géologiques de la Mer Noire. Publ. I.F.P., Géol.* 21773.
- McKenzie, D.P., 1972. Active tectonics of the Mediterranean region. *Geophys. J. R. Astron. Soc.* 30 (109), 109–185.
- Meysner, L.B., Tugolesov, D.A., 1981. Late Cenozoic troughs on the floor of the northeastern Black Sea. *Geotectonics.* 15 (6), 538–545.
- Mileev, V.S., Vishnevskiy, L.Ye., Nikishin, A.M., Rozanov, S.B., 1992. *Formatsii akkretionnoy prizmy Gornogo Kryma (Formation of accretionary prism of Mountain Crimea)*. *Izv. Vuzov. Geol. Razvedka* 4, 25–31.
- Mileev, V.S., Baraboshkin, E.Yu., Nikitin, M.Yu., Rozanov, S.B., Shalimov, I.V., 1996. Evidence that the Upper Jurassic deposits of the Crimean Mountains are allochthons. *Trans. Russian Acad. Sci., Earth Sci. Sect.* 342 (4), 121–124.
- Mileev, V.S., Rozanov, S.B., Baraboshkin, E.Yu., Shalimov, I.V., 1997. The tectonic structure and evolution of the Moun-

- tain Crimea. In: Milanovsky, E.E., Milejev, V.S., Nikishin, A.M., Sokolov, B.A. (Eds.), *Geological Study of Crimea (Otcherki Geologii Krima)*. Geological Faculty MSU Publishers, Moscow, 265, pp. 187–206.
- Morgunov, Yu.G., Kalinin, A.V., Kalinin, V.V., Kuprin, P.N., Limonov, A.F., Pivovarov, B.L., Shcherbakov, F.A., 1979. The principal elements in the tectonics of the southern flank of the Crimean meganticlinorium. *Geotectonics* 13 (4), 310–315.
- Muratov, M.V., 1960. *Kratkiy otcherk geologicheskogo stroeniya Krymskogo polouostrova* (Short geological review of Crimea peninsula). Moscow, gosudarstvenoe nauchno tekhnicheskoe izdatelstvo literaturi po geologii i okhrane nedr, 206 pp.
- Muratov, M.V. (Ed.), 1969. *Geology of the U.S.S.R., VIII. Crimea, Part 1. Geology (in Russian)*. Nedra, Moscow, 576 pp.
- Nikishin, A.M., Cloetingh, S., Baraboshkin, E.Yu., Bolotov, S.N., Kopaeovich, L.F., Nazarevich, B.P., Panov, D.I., Brunet, M.F., Ershov, A.V., Kosova, S.S., Il'ina, V.V., Stephenson, R.A., 1998. Scythian platform: chronostratigraphy and stages of tectonic history. In: Barrier, E., Crasquin, S. (Eds.), *Peri-Tethys Memoir 3, Mém. Mus. Natl. Hist. Nat., Paris 177*, 151–162.
- Nowroozi, A.A., 1972. Focal mechanism of earthquakes in Persia, Turkey, West Pakistan, and Afghanistan and plate tectonics of the Middle East. *Bull. Seismol. Soc. Am.* 62 (3), 823–850.
- Obert, D., Deffontaine, B., Gely, J.P., 1992. Adaptation du réseau hydrographique aux structures et à l'évolution néotectonique, application au Bassin Parisien. *Bull. Inf. Géol. Bass. Paris* 29 (4), 85–95.
- Popadyuk, I.V., Smirnov, S.Y., 1991. Crimea orogen: a nappe interpretation. In: Ziegler, P., Horvath, F. (Eds.), *Peri-Tethys Memoir 2, Structure and Prospects of Alpine Basins and Forelands. Mém. Mus. Natl. Hist. Nat., Paris 170*, pp. 513–524.
- Popadyuk, I.V., Smirnov, S.Y., 1996. The problem of the structure of the Crimean Mountain region: traditional ideas and reality. *Geotectonics* 25 (6), 489–497.
- Robinson, A.G., Rudat, J.H., Banks, C.J., Wiles, R.L.F., 1996. Petroleum geology of the Black Sea. *Mar. Pet. Geol.* 13 (2), 195–223.
- Saintot, A., Angelier, J., Goushtchenko, O., Ilyin, A., Rebetsky, Y., Vassiliev, N., Yakovlev, F., Malutin, S., 1995. Paleostress reconstruction and major structures in Crimea and NW-Caucasus. Communication to the EUG VIII, Strasbourg, 9–13 April 1995, Abstr. Suppl. 1, Terra Nova 7, 269.
- Saintot, A., Angelier, J., Ilyin, A., 1996a. Champs de contraintes en Crimée et dans le Caucase nord-occidentale. 16th Earth Sciences meeting, 10–12 April 1996, Orléans, Abstr. Vol., S.G.F., Paris.
- Saintot, A., Angelier, J., Ilyin, A., 1996b. Reconstruction of Mesozoic–Cenozoic paleostress fields in Crimea and NW-Caucasus: relationships with major structure. Europrobe/Intas Georift Yalta '96 Workshop, GURZUF, 31 Oct.–7 Nov. 1996, *Geophys. J. (Kiev)*, Abstr. 19 (1), 146.
- Saintot, A., Angelier, J., Ilyin, A., Goushtchenko, O., 1998. Reconstruction of paleostress fields in Crimea and the NW-Caucasus: relation with major structure. In: Barrier, E., Crasquin, S. (Eds.), *Peri-Tethys Memoir 3. Mém. Mus. Natl. Hist. Nat., Paris 177*, 89–112.
- Scherba, I.G., 1978. Pliocen–Chervertichnye olistostromy Kryma i mekanizm ikh obrazovanya (Pliocene–Quaternary olistostromes of the Crimea and mechanism of their origin). *Bull. MOIP. Otd. Geol.* 53 (4), 23–34.
- Seismotectonic Map of Iran, Afghanistan and Pakistan, 1984. In: Haghypour, A., Ghorashi, M., Kadjar, M.H. (Eds.), *Geol. Surv. Iran, Teheran*.
- Shreider, A.A., Kazmin, V.G., Lygin, V.S., 1997. Magnetic anomalies and age of the Black Sea Deep Basins. *Geotectonics* 31 (1), 54–64.
- Terekhov, A.A., Shimkus, K.M., 1989. Young sediments and young overthrust structures in the Peri-Crimean and Peri-Caucasus zones of the Black Sea Basin. *Geotectonics* 23 (1), 54–59.
- Tugolesov, D.A., Gorshkov, A.S., Meysner, L.B., Solov'yev, V.V., Khakhalev, Ye.M., 1985. The tectonics of the Black Sea trough. *Geotectonics* 19 (6), 435–445.
- Zonenshain, L.P., Le Pichon, X., 1986. Deep basins of the Black sea and Caspian Sea as remnants of Mesozoic back-arc basins. *Tectonophysics* 123, 181–211.